Published online 20 December 2021

Nucleic Acids Research, 2022, Vol. 50, No. 1 ***259–280***
https://doi.org/10.1093/nar/gkab1225

Canonical and novel non-canonical activities of the Holliday junction resolvase Yen1

Raquel Carreira†, F. Javier Aguado†, Vanesa Hurtado-Nieves and Miguel G. Blanco*

Department of Biochemistry and Molecular Biology, CIMUS, Universidade de Santiago de Compostela-Instituto de Investigación Sanitaria (IDIS), Santiago de Compostela, A Coruña 15782, Spain

Received September 21, 2021; Revised November 12, 2021; Editorial Decision November 24, 2021; Accepted December 01, 2021

Downloaded from https://academic.oup.com/nar/article/50/1/259/6470689 by Irene Ruiz user on 01 July 2022

ABSTRACT

Yen1 and GEN1 are members of the Rad2/XPG family of nucleases that were identified as the first canonical nuclear Holliday junction (HJ) resolvases in budding yeast and humans due to their ability to introduce two symmetric, coordinated incisions on opposite strands of the HJ, yielding nicked DNA products that could be readily ligated. While GEN1 has been extensively characterized *in vitro*, much less is known about the biochemistry of Yen1. Here, we have performed the first in-depth characterization of purified Yen1. We confirmed that Yen1 resembles GEN1 in many aspects, including range of substrates targeted, position of most incisions they produce or the increase in the first incision rate by assembly of a dimer on a HJ, despite minor differences. However, we demonstrate that Yen1 is endowed with additional nuclease activities, like a nick-specific 5′-3′ exonuclease or HJ arm-chopping that could apparently blur its classification as a canonical HJ resolvase. Despite this, we show that Yen1 fulfils the requirements of a canonical HJ resolvase and hypothesize that its wider array of nuclease activities might contribute to its function in the removal of persistent recombination or replication intermediates.

INTRODUCTION

Holliday junctions (HJs) are four-way secondary DNA structures where two duplexes exchange a pair of single strands. HJs and similar cruciform structures may arise during the processes of double-strand break (DSB) repair by homologous recombination (HR), post-replication repair or during the reversal of stalled replication forks. Due to the physical linkage that HJs establish between two DNA molecules, their persistence until late stages of the cell cycle may compromise the correct segregation of sister chromatids or homologous chromosomes in both the mitotic and meiotic scenarios (1). Hence, eukaryotic cells are endowed with two main pathways to ensure their timely removal and the disengagement of the two DNA molecules. First, the combined actions of a RecQ-family helicase Sgs1 in *Saccharomyces cerevisiae* (BLM in mammals), the type IA topoisomerase Top3 (TOPOIIIa) and the OB-fold containing accessory protein Rmi1 (RMI1/RMI2) drive the convergent branch migration of two HJs and fuse them into a hemicatenane structure that can be subsequently decatenated. This process, double HJ dissolution, leads to the formation of non-crossover (NCO) products, exclusively (2). Second, structure-selective endonucleases (SSEs) like *S. cerevisiae* Mus81–Mms4, Slx1–Slx4 and Yen1 (MUS81–EME1/EME2, SLX1–SLX4 and GEN1) can cleave these HJs in a process generally referred to as HJ resolution, which may yield both NCOs and crossover (CO) depending on the orientation of the cuts across the HJs (3–15). Additionally, a fourth nuclease, Mlh1–Mlh3, plays a major role in the resolution of double HJs into COs to ensure chiasmata formation and accurate segregation of homologous chromosomes during meiosis I (16–21).

All these SSEs with the ability to cleave HJs are generally termed HJ resolvases. The extensive biochemical characterization of phage, prokaryotic and mitochondrial resolvases, like T4 Endo VII, T7 Endo I, *Escherichia coli* RuvC, *S. cerevisiae* Cce1 or *Schizosaccharomyces pombe* Ydc2 defined the paradigm of 'canonical' HJ resolution, whereby the enzyme introduces a pair of symmetric, coordinated nicks in opposite strands across the junction, yielding two nicked DNA duplexes that can be directly ligated without further processing (22–39). The two incisions take place within the lifetime of the protein-DNA complex, with the first one being the limiting step of the reaction and greatly accelerating the second cut (40–42). Resolvases that follow this mode of HJ resolution have been dubbed canonical resolvases. Oppositely, non-canonical resolvases typically sever HJs by non-coordinated, asymmetrical incisions that release DNA molecules containing small gaps or flaps, thus requiring additional processing before re-ligation (43).

Yen1 and GEN1 were identified as the first eukaryotic, nuclear SSEs displaying canonical HJ resolvase activity in

*To whom correspondence should be addressed. Tel: +34 881 815 386; Fax: +34 881 815 403; Email: miguel.gonzalez.blanco@usc.es
†The authors wish it to be known that, in their opinion, the first two authors should be regarded as Joint First Authors.

© The Author(s) 2021. Published by Oxford University Press on behalf of Nucleic Acids Research.
This is an Open Access article distributed under the terms of the Creative Commons Attribution-NonCommercial License (http://creativecommons.org/licenses/by-nc/4.0/), which permits non-commercial re-use, distribution, and reproduction in any medium, provided the original work is properly cited. For commercial re-use, please contact journals.permissions@oup.com

budding yeast and humans, respectively (10). Both belong to the subclass IV of the Rad2/XPG family of SSEs and orthologous proteins are present in most organisms analysed, with the notable exception of *S. pombe* (10,44–49). These enzymes are characterized by the presence of a bi-partite nuclease domain (XPG-N/XPG-I), a conserved helix-hairpin-helix motif and a DNA interaction area mediated by a chromodomain, identified both in the human and *Chaetomium thermophilum* orthologs (50–52) (Figure 1A). The biochemical analysis of various members of this subclass IV in humans, nematodes, flies, fungi and plants indicate that all these nucleases retain the characteristic 5′-flap nuclease activity of the Rad2/XPG family, but in most cases have also evolved the ability to resolve HJs in a RuvC-like manner and to process other branched DNA structures like model replication forks and nicked HJs (10,45–50,52–58).

In budding yeast, the role of Yen1 in resolution of HR intermediates has been considerably studied. While deletion of *YEN1* confers no overt DNA repair defects either on its own or in the absence of other members of the Rad2/XPG family of nucleases, it dramatically increases the DNA damage sensitivity of *mus81Δ* and *mms4Δ* mutants (59–63). Yen1 seems dispensable in meiotic recombination, but double *mus81Δ yen1Δ* mutants display meiotic chromosome segregation abnormalities and cannot sporulate (19,59,64–66). These observations have consequently led to the interpretation that Yen1 acts as a back-up mechanism for Mus81-Mms4 in the removal of mitotic and meiotic recombination intermediates. However, it has been recently shown that Yen1 also has a specific role, non-redundant with Mus81-Mms4 or Slx1–Slx4, in the processing of replication intermediates that persist in the absence of the nuclease/helicase Dna2 (67,68). Additionally, it has been shown that Yen1 subcellular localization, catalytic activity and chromatin accumulation are strictly controlled by post-translational modifications. Phosphorylation of Yen1 by the Cdc28 (CDK) kinase both reduces its DNA binding activity and promotes its export to the cytoplasm in S-phase. At the onset of anaphase, the activation of the Cdc14 phosphatase reverts this modification and allows Yen1 activation and re-ingression into the nucleus, where it acts to remove persistent recombination intermediates prior to cell division (64,69–71). Yen1 can also be a substrate for the SUMO ligases Siz1 and Siz2 and the SUMO-targeted ubiquitin ligase Slx5-Slx8 after DNA damage, which drive its polyubiquitination and subsequent proteasomal degradation before entry in S-phase (72). Arguably, these different layers of Yen1 regulation prevent it from severing branched replication and recombination intermediates from S-phase until anaphase, limiting its action to persistent branched DNA intermediates in late stages of mitosis. In this sense, Yen1 mutants that bypass these regulatory mechanisms, such as Yen1^{ON} (69) (identical to Yen1^{9A} (70)) or Yen1^{K714R} (72) have proved extremely useful to ascertain the cellular consequences of premature activation or nuclear persistence of this resolvase. In particular, Yen1^{ON} has been widely employed in different experimental set-ups to uncouple the nucleolytic processing of HR intermediates from cell cycle progression in both mitotic and meiotic contexts. These studies have collectively revealed that in wild-type cells the precise timing of Yen1 activation is essential to minimize genome instability, CO formation and loss-of heterozygosity during mitosis and to properly establish CO interference during meiosis I. Contrarily, in mutants deficient in the processing of HR or replication intermediates, the sustained activation of Yen1^{ON} alleviates or suppresses the phenotypes associated to the toxic accumulation of replication or recombination intermediates (68,69,73–80).

Despite these advances in our understanding of Yen1 functions and regulation, our knowledge about its biochemical properties is relatively lacking compared to some of its orthologs in other organisms, as it mainly derives from its initial identification as a canonical resolvase employing whole-cell extracts (10) and a basic description of its two activation states once the protein was successfully purified (69). Here, we present an analysis of Yen1 biochemical properties, with a special focus in the characterization of its activities as a canonical HJ resolvase. Our results reveal that, despite its general behaviour as a bona-fide canonical HJ resolvase, Yen1 is endowed with additional nucleolytic activities that may blur this adscription, at least according to its *in vitro* properties. In this sense, we have identified a novel nick-specific 5′-3′exonuclease activity that renders Yen1 resolution products unable to be ligated as well as an alternative, non-canonical two-step mode of HJ processing, which we term 'arm-chopping'. Additionally, we have discovered that despite their many similarities, Yen1 and human GEN1 display different preferences for HJ strand cleavage. We speculate that such activities might contribute to the processing of particularly recalcitrant branched DNA intermediates, but also account for the detrimental effects of its premature activation.

MATERIALS AND METHODS

Plasmids and strains

All *S. cerevisiae* strains and plasmids employed are described in Supplementary Tables S1 and S2, respectively.

The coding sequence of *YEN1^{WT}* in p416ADH1-YEN1^{WT}-V5-6xHis (60) was mutagenized and/or subcloned into p416GPD1 (81) to create p416ADH1-YEN1^{ON}-V5-6xHis, p416GPD1-YEN1^{WT}-V5-6xHis and p416GPD1-YEN1^{ON}-V5-6xHis. The vector pENTR221-GEN1^{WT}-FTH-STOP, a kind gift from Gary Chan and Stephen C. West that contains the coding sequence of C-terminally tagged GEN1^{WT}-3xFLAG-2xTEV-10xHis (FTH tag), was modified by site-directed mutagenesis and inverse PCR to generate pENTR221-GEN1^{nuc}-FTH-STOP, which encodes a constitutive nuclear form of GEN1 by mutation of its nuclear export signal and addition of 3xSV40 nuclear localization signals (54). From these two vectors, derivative plasmids carrying either full length or truncated (1-527) versions of GEN1^{WT} or GEN1^{nuc} (pENTR221-GEN1$^{WT/nuc}$-GO, pYES-EXP52-GEN1$^{WT/nuc}$-V5-6xHis and pYES-EXP52-GEN1$^{1\text{-}527\ WT/nuc}$-V5-6xHis, pAG306GAL-GEN1-FTH) were created by standard subcloning, inverse PCR and/or Gateway recombination. Details of each cloning can be provided upon request.

Downloaded from https://academic.oup.com/nar/article/50/1/259/6470689 by Irene Ruiz user on 01 July 2022

Genotoxicity assays

Yeast strains were grown to mid-logarithmic phase in SC-URA containing 2% glucose. The cultures were then normalized to an $OD_{600} = 0.5$ and 10-fold serial dilutions were spotted onto fresh SC-URA plates containing 1% raffinose, 2% galactose and increasing concentrations of methyl methanesulfonate (MMS). Plates were incubated in the dark for 3 days at 30°C and then photographed in a Gel Doc XR+ (Bio-Rad).

Immunofluorescence microscopy

Strains carrying V5-tagged versions of Yen1 or GEN1, either in a wild-type or *mus81Δ yen1Δ* background (Supplementary Table S1), were cultured in SC-URA for 16 h at 30°C, then diluted to an $OD_{600} = 0.2$ in fresh medium and incubated for 5 h. Cells were then fixed by addition of 0.1 vol formaldehyde and incubation at 4°C overnight. Cells were washed once in 0.1 M phosphate buffer pH 7.4, once in spheroplasting buffer (0.1 M phosphate buffer pH 7.4, 0.5 mM $MgCl_2$ and 1.2 M sorbitol) and then incubated in 200 μl of spheroplasting buffer containing 28 mM β-mercaptoethanol at 30°C for 15 min. 100-T Zymolyase (AMSBIO) was added to a final concentration of 1 mg/ml and incubated at 30°C for an additional 10 min. Spheroplasts were then attached to a polylysine-coated multi-well microscope slide and dehydrated in consecutive methanol and acetone baths at –20°C. Slides were blocked for 30 min at RT in PBS containing 1% BSA and then incubated with mouse monoclonal anti-V5 antibodies (1:200 dilution, Invitrogen #R960-25) at 25°C for 1 h. After washing with PBS–BSA, the slides were incubated with an Alexa Fluor 488-coupled anti-mouse antibody from goat (1:200 dilution, Life technologies #A-11001). DNA was stained with DAPI. Images were acquired using a confocal microscope Leica TCS SP8 with HC PL APO CS2 63×/1.40 OIL lens, under the control of LAX software.

Protein purification

Wild-type Yen1, deregulated $Yen1^{ON}$ and catalytically inactive $Yen1^{ND}$ (E193A, E195A) were all purified from yeast as fusions with a C-terminal 3xFLAG-2xTEV-10xHIS (FTH) tag, as previously described (69,82). $Yen1^{P}$ and $Yen1^{ON\text{-}P}$ represent a highly phosphorylated version of the protein, purified from cells arrested at restrictive temperature before anaphase entry in a *cdc14-1* strain. $Yen1^{\lambda}$ and $Yen1^{ON\text{-}\lambda}$ are lambda phosphatase-treated versions of $Yen1^{P}$ and $Yen1^{ON\text{-}P}$ respectively (69). A lambda phosphatase-treated version of $Yen1^{ND}$ was used as catalytically inactive mutant, except in Supplementary Figure S8. For control reactions with FTH-tagged GEN1 or $GEN1^{1–527}$, samples for initial experiments were kindly provided by Gary Chan and Stephen C. West. Additional batches were purified as described (40). All protein batches were tested for non-specific exonuclease, endonuclease and protease contaminant activities and analysed by SDS-PAGE through Novex Value 4–20% Tris-Glycine Mini Gel (Thermo Fisher Scientific) followed by Coomassie staining.

Protein analysis

For the preparation of soluble protein lysates containing Yen1 or GEN1, strains expressing different versions of V5-tagged Yen1 or GEN1 were cultured in 15 ml SC-URA supplemented with 2% glucose. When a density of $\sim 0.6 \times 10^7$ cells/ml was reached, cells were harvested, rinsed in water, and resuspended in 15 ml SC-URA containing 1% raffinose and 2% galactose and incubated for 6 h at 30°C to induce protein expression. Cells were then harvested and resuspended in lysis buffer (40 mM Tris–HCl pH 7.5, 150 mM NaCl, 10% glycerol, 0.10% NP-40, 1 mM DTT, 1 mM PMSF, 5 mM NaF, 5 mM H_2NaPO_4, 5 mM β-glycerophosphate) and disrupted using a Mini-Beadbeater-16 (BioSpec). Lysates were quantified with the Bradford reagent method (BioRad) and normalized to 2 mg/ml. Protein expression levels were assessed by western blotting employing an anti-V5 antibody (1:3000 dilution, Invitrogen, #R960-25).

Mobility-shift detection of phosphorylated Yen1 variants by western-blotting was performed by separating 400 ng of purified $Yen1^{P}$, $Yen1^{\lambda}$, $Yen1^{ON\text{-}P}$ and $Yen1^{ON\text{-}\lambda}$ through 7.5% SDS-PAGE gels, either unmodified or containing 40 μM Phos-tag (Wako Chemicals) and 160 μM $MnCl_2$. Prior to transference, Phos-tag gels were washed with transfer buffer (192 mM glycine, 25 mM Tris-Base, 0,02% SDS, 20% methanol) containing 100 mM EDTA for 30 min at RT, and then washed 3 × 15 min with transfer buffer. Proteins were detected with anti-FLAG M2-HRP (1:3000 dilution, Sigma #A8592).

Hydrodynamic analysis of Yen1

Glycerol gradient sedimentation and size exclusion chromatography were carried out essentially as described (56), with the following modifications. 25 μg $Yen1^{\lambda}$ was loaded on 15–35% glycerol gradients prepared in 40 mM Tris–HCl, pH 7.5, 500 mM NaCl, 0.1% NP-40 and 1 mM DTT. For size exclusion chromatography, 20 μg $Yen1^{\lambda}$ was applied to a Superdex 200 PC 3.2/30 column (GE Healthcare) in the same buffer. In both cases, the fractions collected were analysed by SDS-PAGE through 4–12% MOPS NuPage gradient gels (Thermo Fisher Scientific) followed by Coomassie staining.

DNA substrates

Synthetic substrates were prepared essentially as described (82), employing PAGE-purified ssDNA oligonucleotides. All the oligonucleotides are listed in Supplementary Table S3 and the strand composition of each substrate is described in Supplementary Figure S1. Briefly, labelled and unlabelled oligonucleotides were mixed in a 1:3 ratio, boiled in a water bath, cooled down to room temperature overnight and fully ligated substrates were purified from 10% polyacrylamide gels. For radioactive substrates, oligos were either 5′-end-labelled with [γ-^{32}P]-ATP (3000 Ci/mmol, Perkin Elmer) and T4 PNK (Thermo Fisher) or 3′-end-labelled with [α-^{32}P]-cordycepin (3000 Ci/mmol, Perkin Elmer) and terminal transferase (New England Biolabs). For fluorescent substrates, 5′-IRDye 700, 5′-IRDye 800-labelled (Integrated DNA Technologies), 5′-6FAM or 3′-6FAM-labelled

Downloaded from https://academic.oup.com/nar/article/50/1/259/6470689 by Irene Ruiz user on 01 July 2022

oligonucleotides (Sigma-Aldrich) were employed. For biotinylated substrates, 5′-biot-X01 oligonucleotide (Sigma-Aldrich) was employed. Unlabelled substrates were prepared with equimolecular mixtures of oligonucleotides and purified from native 10% polyacrylamide gels by UV-shadowing. When appropriate, oligonucleotides containing one or three consecutive phosphorothioate (SP) linkages (Sigma-Aldrich) were employed.

Mapping of cleavage sites of various DNA substrates

For the mapping of the incisions on each oligonucleotide (Figures 1, 2, Supplementary Figures S3 and S4), 5 nM protein was incubated with 20 nM unlabelled substrate (unless otherwise stated) supplemented with ∼0.1 nM 5′-^{32}P-end-labelled substrate in 25 μl of reaction buffer (Yen1 reaction buffer: 50 mM Tris–HCl pH 7.5, 0.5 mM $MgCl_2$; GEN1 reaction buffer: 50 mM Tris–HCl pH 7.5, 1 mM $MgCl_2$, 1 mM DTT). In all reactions, enzymes represent 1/10 of the final volume (or enzyme storage buffer in mock reactions). After 10 min of incubation at 30°C (Yen1ND, Yen1^{P} or Yen1$^{\lambda}$) or 37°C (GEN1$^{1\text{-}527}$), 10 μl of each reaction were deproteinized by addition of 2.5 μl stop solution (2% SDS, 10 mg/ml proteinase K) and incubation at 37°C for 20 min, followed by addition of 0.2 vol of 6× native loading buffer (15% Ficoll-400, 60 mM EDTA, 19.8 mM Tris–HCl pH 8.0, 0.48% SDS). Another aliquot of 10 μl was mixed with 1 vol of 2× denaturing loading buffer (TBE 1×, 80% formamide) and incubated at 99°C for 3 min. The radiolabelled products were then separated by PAGE through 10% native or denaturing (7 M urea) gels. Radiolabelled molecules were analysed by phosphorimaging using a Typhoon FLA 9500 and quantified by densitometry using ImageQuant software (GE Healthcare).

Nuclease time-courses experiments

Time-course experiments for Yen1^{P} and Yen1$^{\lambda}$ (Supplementary Figure S2) were carried out by pre-incubation of 5 nM 5′-6FAM fluorescent DNA substrate (5′-flap (5′F), replication fork (RF), nicked X0 HJ (X0n3) and fully ligated X0 HJ (X0)) with increasing concentrations of Yen1^{P} or Yen1$^{\lambda}$ (25, 50, 100, 200 or 500 nM) in Yen1 reaction buffer (as described in 'Mapping of cleavage sites of various DNA substrates') without $MgCl_2$ for 5 min at 4°C. Cleavage was initiated by addition of 0.5 mM $MgCl_2$ and incubation at 30°C. Aliquots were taken at each time point (0, 15, 30, 45, 60, 75, 90, 105 and 120 s) and stopped by addition of 2.5 μl stop solution and incubation at 37°C for 30 min. These likely represent single turn-over conditions for Yen1$^{\lambda}$ in most cases, but not for Yen1^{P}. Products were separated through 10% native PAGE, scanned at 488 nm in a Typhoon FLA 9500 and quantified by densitometry using ImageQuant software. Each time-course was carried out three times independently. To estimate apparent reaction rates (k_{obs}) at various enzyme concentrations, we assumed pseudo-first order kinetics and fitted the fraction of cleaved DNA at time t by non-linear regression as described elsewhere (48) using GraphPad Prism.

Time-course experiments in Supplementary Figure S9 were carried out in duplicates, using 50 nM 5′-IRDye-800 fluorescent DNA substrates and 40 nM Yen1^{P}, Yen1$^{\lambda}$, Yen1$^{ON\text{-}P}$ or Yen1$^{ON\text{-}\lambda}$ for reactions with X0 HJ or RF and 10 nM enzyme in those with the 5′-flap. Reactions were incubated in Yen1 reaction buffer (as described in 'Mapping of cleavage sites of various DNA substrates') at 30°C, aliquots were taken at each time point and stopped by addition of 2.5 μl stop solution further incubation at 37°C for 30 min. Products were separated through 10% native PAGE and analysed using an Odyssey infrared imaging system (LI-COR Biosciences).

Symmetricity of cleavage

To assess if Yen1 was capable of symmetrical resolution of a HJ (Figure 3), we employed an X0 HJ with three hydrolysis-resistant phosphorothioate linkages between nucleotides 30 to 33 in strands X0-2 and X0-4 (HJ-2SP). Reactions were carried out as described for the mapping analyses. 5 nM unlabelled HJ or HJ-2SP spiked with ∼0.5 nM each 5′-^{32}P-end-labelled junction was incubated with 5 nM Yen1$^{\lambda}$ (30°C, 30 min) or 5 nM GEN1$^{1\text{-}527}$ (37°C, 2.5 min). The radiolabelled products were then separated by PAGE through 10% native or denaturing (7 M urea) gels. Radiolabelled molecules were analysed by phosphorimaging using a Typhoon FLA 9500 and quantified by densitometry using ImageQuant software. Reactions in Figure 3D were carried out in triplicate.

Preference for axis cleavage

To assess any preference for the axis of HJ resolution (Figure 4), reactions were carried out as described for the mapping analyses. 5 nM unlabelled J3 HJ spiked with ∼0.5 nM 5′-^{32}P-end-labelled junction was incubated with 50 nM Yen1$^{\lambda}$ (30°C, 5 min) or 5 nM GEN1 (37°C, 5 min). The radiolabelled products were separated by 10% denaturing PAGE and quantified by phosphorimaging as described. The experiment was carried out in triplicate.

Re-ligation and exonuclease activity experiments

For re-ligation experiments (Figure 5B and F), ∼0.5 nM 5′-^{32}P-end-labelled asymmetric HJ X1-T (40) or X1-T-SP were incubated with 10 nM Yen1$^{\lambda}$ or GEN1 for 30 min under the same conditions described for the mapping analysis. 10 μl aliquots of each reaction were either left untreated or adjusted to 1X T4 DNA ligase buffer, supplemented with 5 U of T4 DNA ligase (Fisher, #EL0014) and further incubated for 1 h at 25°C. All reactions were stopped by adding 1 vol of 2× denaturing loading buffer and incubated at 99°C for 3 min. Products were then analysed by 10% denaturing PAGE and phosphorimaging as described above.

For exonuclease assays in Figure 5C and D, ∼0.5 nM either 5′- or 3′- ^{32}P-end-labelled nicked or gapped dsDNA substrates were incubated with increasing concentrations of Yen1$^{\lambda}$ (0, 0.25, 0.5, 1, 2, 4, 8 nM in Figure 5C; 0, 0.5, 2, 8 nM in Figure 5D) for 10 min at 30°C in Yen1 reaction buffer (as described in 'Mapping of cleavage sites of various DNA substrates') in a total volume of 20 μl. After incubation, all reactions were stopped with 5 μl stop buffer, 37°C, 1 h. For analysis under native conditions, reactions were mixed with 0.2 vol of 6× native loading buffer and separated in

Downloaded from https://academic.oup.com/nar/article/50/1/259/6470689 by Irene Ruiz user on 01 July 2022

10% PAGE native gels. For analysis under denaturing conditions, reactions were mixed with 1 vol of 2× denaturing loading buffer, boiled and loaded on 12% PAGE gels containing 7 M urea. Gels were analysed by phosphorimaging as described before.

For exonuclease experiments in Figures 5E and Supplementary Figure S6C, 50 nM enzyme was incubated on its reaction buffer with 10 nM 3′-6FAM-fluorescent substrates for 10 min at 30°C for Yen1$^{\lambda}$ and Yen1ND and 37°C for GEN1. After incubation, all reactions were mixed with 1 vol of 2× denaturing loading buffer, boiled, loaded on 13% PAGE gels containing 7 M urea and scanned at 488 nm in a Typhoon FLA 9500. For exonuclease experiments performed at different temperatures (Supplementary Figure S6A and B), 2 nM Yen1$^{\lambda}$ or Yen1ND was incubated in Yen1 reaction buffer (as described in 'Mapping of cleavage sites of various DNA substrates') with 10 nM 3′-6FAM-nicked dsDNA or 5′-6FAM-5′flap at the indicated temperatures (20, 25, 30, 35, 40 and 45°C) for 5 min (5′-flap) or 20 min (nicked dsDNA). Reactions were processed as stated above. Gels were scanned at 488 nm in a Typhoon FLA 9500 and quantified by densitometry using ImageQuant software. Experiments in Supplementary Figure S6A were done three independent times.

Cruciform assays

In experiments with the cruciform-forming pIR9 plasmid (47) (Figure 6B), extrusion of the cruciform was favored by preincubation at 37°C in extrusion buffer (50 mM Tris–HCl pH 7.5, 50 mM NaCl, 0.1 mM EDTA). Cruciform cleavage assays were carried out in 10 μl Yen1 reaction buffer (as described in 'Mapping of cleavage sites of various DNA substrates') containing 4.5 nM plasmid and 90 nM Yen1^{P} or Yen1$^{\lambda}$ at 30°C. Aliquots were taken at 0, 7.5, 15, 30, 60, 90 and 120 min. Resistance to digestion by EcoRI was employed to measure cruciform extrusion levels. Products were separated in 0.8% agarose gels, stained with ethidium bromide, and imaged and quantified on a Gel Doc XR + System using the Image Lab software (Bio-Rad). Each experiment was done three independent times.

For the ligation experiment in Figure 6C, 4.5 nM pIR9 was incubated with 90 nM Yen1^{P} in Yen1 reaction buffer for 1 h at 30°C. In addition, incubation of the cruciform plasmid with 10 U Nt.BspQI (NEB) at 50°C for 1 h was used as a control for a nicked circle. After the nuclease reaction, the DNA was purified using a commercial kit (E.Z.N.A.Cycle-Pure Kit, Omega Bio-tek #D6492-02). Following the purification, 5 U T4 DNA ligase was added to 100 ng of purified DNA in the supplied ligase buffer for 1 h at 37°C. Products were analysed as stated above.

For experiments in Figure 6D, pIR9 was pre-nicked with Nt.BspQI and purified by phenol-chloroform extraction. After this, 4.5 nM nicked pIR9 was incubated with 90 nM Yen1^{P}, Yen1$^{\lambda}$ or Yen1ND for 90 min at 30°C. After the nuclease reaction, the DNA was purified using commercial DNA purification kits followed by 1 h incubation with 5 U T4 DNA ligase at 37°C. Products were then analysed as stated above.

For the labelling experiments (Figure 6F), 4.5 nM pIR9 was incubated with 90 nM Yen1 (Yen1$^{\lambda}$, Yen1$^{ON\text{-}\lambda}$ or Yen1ND), 50 nM GEN1, 10 U Nt.BspQI or 1 U EcoRI in their corresponding reaction buffers for 90 min. Reactions were carried out in a final volume of 20 μl. After this, they were treated with 1 U thermosensitive alkaline phosphatase (FastAP, Thermo Fisher) for 1 h at 37°C, and inactivated for 5 min at 75°C. Then, half of the reaction was loaded on agarose gels as described, and the other half was denatured at 99°C for 3 min. After this, 50 μl 50 mM Tris–HCl was added to the reaction and applied to a G-25 MicroSpin column. The eluted reaction products were labelled by adding 1 μl [γ-^{32}P]-ATP (3000 Ci/mmol, Perkin Elmer) and 10 U T4 PNK for 1 h at 37°C. The non-incorporated isotope was eliminated using G-25 columns and the eluted DNA was precipitated with 2 vol of ethanol, 0.1 vol of 3 M sodium acetate pH 5.2 and 0.02 vol of 5 mg/ml glycogen. The pellet was resuspended in 10 μl 2× denaturing loading buffer and samples analysed in 15% denaturing gels as described above.

Nicking stimulation by dimer formation

To assess if the dimerization of Yen1 on a HJ favours its first incision, we employed an X0 HJ with a SP linkage between nucleotides 31–32 in strand X0-3 (X0-SP). Experiments in Figure 7B and C were performed as described for the mapping analyses. 5 nM unlabelled substrates were used, and the incubation time was 5 min for Yen1$^{\lambda}$ and 2.5 min for GEN1.

For experiments in Figures 7D, E and Supplementary Figure S8, 10 nM 5′-6FAM-HJ-X0-SP was incubated with 2 nM Yen1$^{\lambda}$ or Yen1^{P} and increasing concentrations of Yen1ND or Yen1$^{ND\text{-}P}$ respectively (0, 4, 8, 16, 32, 64, 128 nM) in Yen1 reaction buffer (as described in 'Mapping of cleavage sites of various DNA substrates'). Reactions were incubated 5 min for Yen1$^{\lambda}$ (Figure 7D, E) or 1 h for Yen1^{P} (Supplementary Figure S8) at 30°C. All reactions were stopped by adding 1 vol of 2× denaturing loading buffer and incubated at 99°C for 3 min. Products were then analysed by 10% denaturing PAGE, scanned at 488 nm in a Typhoon FLA 9500 and quantified by densitometry using ImageQuant software. Each experiment was done three independent times.

For the kinetic analysis in Figure 7F, 2 nM Yen1$^{\lambda}$ was pre-mixed with 0, 32 or 128 nM Yen1ND. Reactions were performed and analysed as described above. Aliquots were taken at 0, 1, 2, 4, 8, 16, 32, 64 and 128 min. Reaction rates were calculated from triplicate time-courses using GraphPad Prism, employing a global adjustment of all the data points to a single exponential curve, assuming a pseudo-first order reaction. Data are presented as the reaction rate in 1/s with a 95% CI. Significance of the difference between reaction rates was estimated by an extra-sum-of-squares F-test.

Bio-layer interferometry assays

Binding kinetics of Yen1$^{\lambda}$ and Yen1ND to a biotinylated X0 HJ were measured by bio-layer interferometry (BLI) using a BLItz instrument (FortéBio). Streptavidin-coated biosensors (FortéBio, Cat No. 18–5019) were pre-hydrated in Yen1 binding buffer (50 mM Tris–HCl pH 7.5, 125 mM NaCl, 5 mM EDTA, 1 mM DTT, 100 μg/ml BSA, 11% glycerol)

Downloaded from https://academic.oup.com/nar/article/50/1/259/6470689 by Irene Ruiz user on 01 July 2022

for 10 min. BLI experiments involved the following steps: (i) baseline establishment, 30 s; (ii) loading 5′-biotinylated X0 HJ, 120 s; (iii) wash in binding buffer, 30 s; (iv) association step with Yen1$^{\lambda}$ or Yen1ND (250, 500 or 1000 nM), 120 s; (v) dissociation step in binding buffer, 120 s. Data Acquisition 9.0 software (FortéBio) was used to record binding events in duplicate experiments and to estimate the equilibrium dissociation constant (K_D). The K_D values obtained for the enzyme-HJ complexes were 5.84 ± 0.60 nM (mean ± SD) with Yen1$^{\lambda}$ and 13.47 ± 1.76 nM with Yen1ND.

Nuclease assays with whole-cell lysates

Nuclease assays with whole-cell lysates from strains expressing Yen1 or GEN1 were performed with 50 nM 5′-IRDye-700 labelled X0 HJ in either Yen1 or GEN1 reaction buffer (as described in 'Mapping of cleavage sites of various DNA substrates'). 1 μl of normalized lysate (∼2 mg/ml total protein) was added to each reaction and incubated for 1 h at 30°C. Products were analysed by 10% native PAGE and gels were scanned using an Odyssey infrared imaging system.

Protein sequence alignment

Protein sequences for GEN1 (Q17RS7), CtGEN1 (G0RYN2) and Yen1 (P40028) were retrieved from Uniprot (83) and aligned with SnapGene software (www.snapgene.com) using Clustal Omega (84). Predicted structural features for Yen1 were retrieved from AlphaFold (85).

RESULTS

Yen1 and GEN1 cleave four- and three-way junctions at similar, but not identical, positions

Yen1 nuclease activity is regulated by CDK-dependent phosphorylation events that inhibit both its overall DNA-binding and catalytic activity (69,70). However, it is not known whether these changes may also alter the position of the incisions that Yen1 creates on the substrates. To investigate this, we purified highly phosphorylated (Yen1^{P}) and *in vitro*, lambda phosphatase-dephosphorylated (Yen1$^{\lambda}$) versions of Yen1 (Figure 1B) and incubated them with X0 HJ, nicked X0 HJ (X0n), replication fork (RF) and 5′-flap (5′F) synthetic DNA substrates. In agreement with previous results (69,70), time-course analyses of Yen1^{P} and Yen1$^{\lambda}$ demonstrated the inhibitory effect of phosphorylation on the processing of all this substrates, being the 5′-flaps and nicked X0 HJs processed more efficiently than replication forks and X0 HJs (Supplementary Figure S2). For the high-resolution mapping of incision sites on various branched DNA structures, including X0 HJs, three-way junctions (3WJ), replication forks and 5′-flap substrates, we separated the reaction products by 7 M urea denaturing PAGE (Figure 1C–F). The same reactions were also analysed by native PAGE (Supplementary Figure S3). We observed that, despite their different efficiency, the incision sites produced by Yen1^{P} and Yen1$^{\lambda}$ on all the tested substrates are entirely coincident, indicating that the upregulation of Yen1 activity by dephosphorylation does not alter its cleavage specificity.

In parallel, we also compared Yen1 incisions with those created by its human homolog GEN1 on the same set of substrates (Figures 1C–G, Supplementary Figures S3 and S4). On the static, fully ligated X0 HJ substrate (10), GEN1 typically introduces symmetrical nicks 1 nt at the 3′ of the branching point specifically on strands X0-1 and X0-3 (Figure 1C and G), in agreement with previous reports (10,40,56). On top of these cuts, Yen1 can nick strands X0-2 and X0-4 of X0 HJ, typically 1 or 2 nt at the 3′ of the branching point. Therefore, it seems that while GEN1 preferentially resolves the X0 HJ over the 1–3 axis, Yen1 can process it across both the 1–3 and 2–4 axis. Interestingly, the analysis of the cleavage products by native PAGE revealed that Yen1, but not GEN1, gives rise to two additional bands apart from the nicked duplex expected by canonical resolution (Supplementary Figure S3). These species migrate in positions comparable to those of a replication fork-like (RF-like) structure and a 30 nt duplex, which would be consistent with the cleavage of two annealing strands, and thus releasing one helical arm of the junction. Differences between the two enzymes in their preference to cleave specific strands can also be observed on a fully continuous 3WJ (Figure 1E and G). For this substrate, Yen1 has a marked preference to incise strand X0-1, again 1 nt at the 3′ of the branching point, while GEN1 produces detectable nicking on all strands of this substrate. Together with the results obtained with the X0 HJ, this suggests that the two enzymes may recognize or remodel these continuous branched substrates in a different manner or, alternatively, that they may display a mild, but slightly different sequence preference for cleavage. However, substrates with discontinuous strands like model replication forks or 5′-flaps were almost exclusively processed by both Yen1 and GEN1 on strand X0-4, 1 or 2 nt at the 3′ from the branching point of the 5′ arm/flap (Figure 1D, F and G). An additional incision 4 nt into the 5′-flap strand for GEN1 that has been previously observed was also recapitulated in our analysis (40). We also tested if Yen1 could nick any of the strands of 3′-flap, splayed arm, double- and single- stranded DNA substrates. In agreement with our previous results showing no cleavage of these structures (69), we did not detect incisions produced by Yen1 on any of their constituent strands (Supplementary Figure S4).

Yen1 can incise both the opposing and 5′ strands of nicked HJs

Nicked HJs are particularly interesting intermediates during HR, as they represent the precursors of fully ligated HJs and are considered in many instances as a key intermediate to generate crossovers (86–89). To specifically assess how Yen1 resolves these structures, we generated the four possible nicked HJs based on the X0 structure (X0n1 to X0n4, with n1–4 indicating the nicked strand) and independently labelled each of the intact strands. The resulting set of 12 substrates was incubated with Yen1 or GEN1 and their incisions mapped as described in the previous section. When we labelled the strand opposing the nick (Figure 2A), we observed that both Yen1 and GEN1 hydrolysed it 1 nt to the 3′-side of the junction point (position 31) for X0n1 and X0n3. In junctions X0n2 and X0n4, Yen1 still cleaves mainly at position 31, but GEN1 does it 1–3 nt to the 3′-side

Downloaded from https://academic.oup.com/nar/article/50/1/259/6470689 by Irene Ruiz user on 01 July 2022

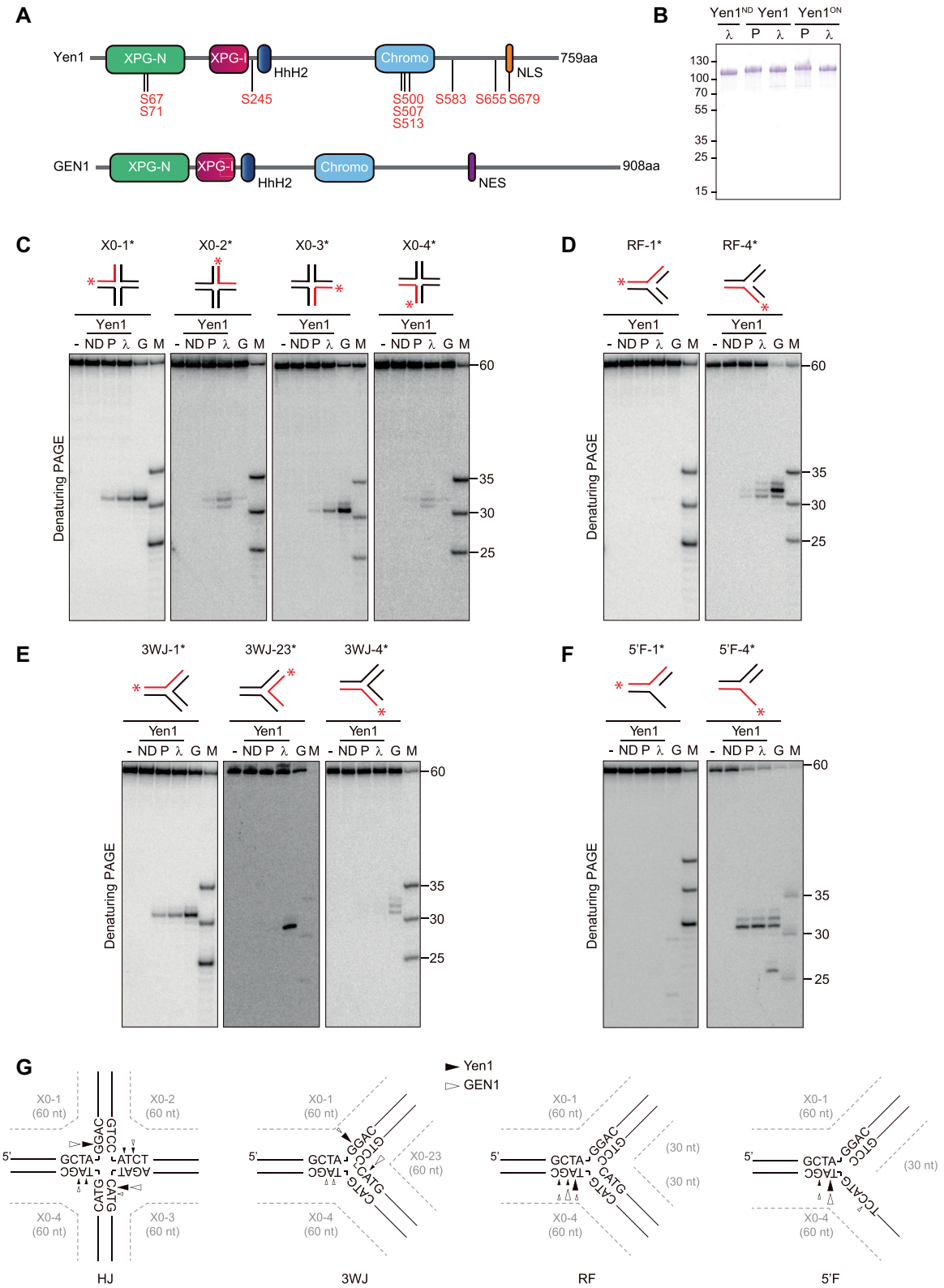

Figure 1. Mapping of Yen1 incisions on branched DNA substrates. (**A**) Graphical representation of Yen1 and GEN1 domains. Serines in consensus CDK phosphorylation sites are indicated in Yen1. (**B**) FTH-tagged Yen1ND, Yen1^{P}, Yen1$^{\lambda}$, Yen1$^{ON\text{-}P}$ and Yen1$^{ON\text{-}\lambda}$ were purified, analysed by SDS-PAGE and stained with Coomassie. Molecular weight markers are indicated in kDa. (**C**) Holliday junction X0 (20 nM) was 5′-end-labelled with ^{32}P (asterisk) on each strand (red) and incubated with 5 nM Yen1ND (ND), Yen1^{P} (P), Yen1$^{\lambda}$ (λ) or GEN1$^{1–527}$ (G) for 10 min at 30°C or 37°C, respectively. (-) indicates no enzyme. Products were analysed by 10% denaturing PAGE and phosphorimaging. A mixture of 5′-^{32}P-end-labelled oligos of defined length (25, 30, 35 and 60 nt) were used as markers (M). (**D–F**) As in (C), employing a (D) replication fork (RF), (E) 3-way junction (3WJ) or (F) 5′-flap (5′F) as a substrate. (**G**) Schematic representation of incision sites identified for the HJ, 3WJ, RF and 5′F substrates. Only the nucleotide sequence near the branch point is shown. Arrow size indicates preferential cleavage sites for Yen1 (black) and GEN1 (white).

Downloaded from https://academic.oup.com/nar/article/50/1/259/6470689 by Irene Ruiz user on 01 July 2022

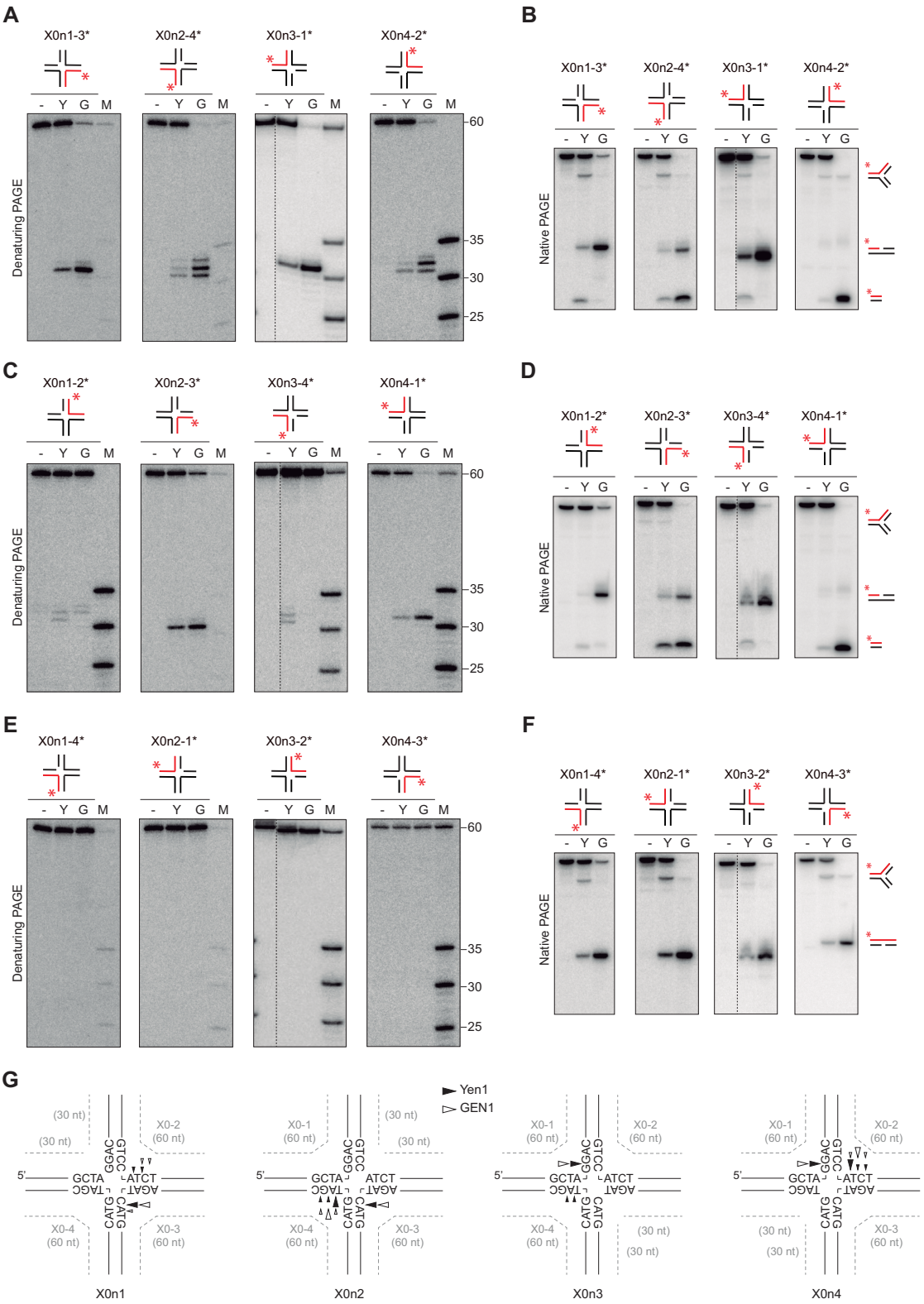

Figure 2. Mapping of Yen1 incisions on nicked HJs. Reactions with different nicked X0 HJs and Yen1$^{\lambda}$ or GEN1$^{1\text{-}527}$ were carried out and labelled as in Figure 1. (**A**) Reactions using nicked X0 substrates labelled on the strand opposite the nick were analysed by 10% denaturing PAGE or (**B**) 10% native PAGE (cleavage products depicted on the right). (**C**, **D**) same as (A, B), but employing nicked X0 substrates labelled on the 5′strand with respect to the nick. (**E**, **F**) same as (A, B), but employing nicked X0 substrates labelled on the 3′strand with respect to the nick. Dotted lines in some gels indicate splicing of superfluous lanes. (**G**) Schematic representation of incision sites identified for the different nicked X0 substrates. Please note the discontinuity of one strand in each of them. Only the nucleotide sequence near the branch point is shown. Arrow size indicates preferential cleavage sites for Yen1 (black) and GEN1 (white).

Downloaded from https://academic.oup.com/nar/article/50/1/259/6470689 by Irene Ruiz user on 01 July 2022

of the junction point, mainly in position 32 of the oligonucleotide (Figure 2A and G). Interestingly, these incisions on the nicked X0 HJ are not perfectly symmetrical to the pre-existing nick in position 30 and thus would lead to duplex products that would contain typically 1 nt (up to 3 nt) gaps or 3′-flaps, as it has been observed for the *Arabidopsis* orthologs (47).

It is generally considered that the presence of a nick in a HJ increases its flexibility and the accessibility of the SSEs for the cleavage of the opposite strand, thus favouring counter-nicking and resolution of the junction (90). Accordingly, analysis of the same reaction products on native gels also revealed that the expected 60 nt duplex resulting from resolution of the X0n1 and X0n3 was almost the exclusive product for GEN1 (Figure 2B). However, in the case of Yen1, the same pattern of 3 bands (RF-like, nicked duplex, small duplex) observed with intact X0 HJ was still present, to different extents, with all the nicked X0 versions. Surprisingly, the major product of GEN1 on X0n2 and X0n4 was the small duplex molecule, which necessarily involves the cleavage of the 5′strand with respect to the nick. Indeed, when we labelled the 5′strand in all the nicked X0 HJs, we detected cleavage by both nucleases in all cases, except for GEN1 on X0n3-4* (Figure 2C and G) and consistently, we observed again the presence of the small duplexes in the native gels, except for X0n3-4* (Figure 2D). Conversely, we detected no incisions or the presence of the small duplex product when the nicked junctions were labelled on the 3′strand with respect to the nick (Figure 2E, F and G).

The removal of one arm from a nicked HJ to produce a three-arm structure has already been observed for the *A. thaliana* orthologs of Yen1, AtGEN1 and AtSEND1 (47), being referred to as *Ref-I* (Replication Fork Intermediate) activity. Interestingly, the small duplex that we observe when we label the strand opposite the nick (Figure 2B) cannot directly arise as a consequence of this *Ref-I* activity. Instead, it must involve a sequential reaction, in which the first incision by *Ref-I* activity on the 5′strand with respect to the nick is followed by a second incision on the resulting RF-like intermediate, with the typical 5′ polarity of the Rad2/XPG family (Supplementary Figure S5A).

Both symmetrical resolution and arm-chopping contribute to the formation of nicked duplex DNA from a synthetic HJ

The paradigm of canonical HJ resolution proposes that two symmetrical, coordinated incisions across the axis of the HJ produce a pair of nicked duplexes (23,91). Surprisingly, when we analysed the cleavage products generated by Yen1 on an intact X0 HJ in native gels (Supplementary Figure S3), we detected the formation of, apparently, the same two additional species that we observed with the nicked X0 HJs: one with a migration compatible with a RF-like structure and another migrating like a small (∼30 nt) DNA duplex.

This suggests that Yen1 may exhibit an alternative way of processing an intact HJ: the cleavage of both strands in one arm of the HJ, releasing a small dsDNA fragment and a RF-like, three-arm structure (Supplementary Figure S5B). This arm-chopping activity can also be observed in some of Yen1 orthologs such as AtGEN1 and AtSEND1 (47), OsGEN1 (58) and DmGEN1 (53). Importantly, the RF-like structure produced by this arm-chopping would be susceptible of further processing to yield a nicked dsDNA product, similar to the one expected by symmetrical resolution, in a situation analogous to that described for the *Ref-I* activity on nicked HJs (Supplementary Figure S5A). This poses an interesting caveat: is Yen1 able to symmetrically resolve an intact HJ into two nicked dsDNA molecules or do these nicked duplexes arise from a two-step mechanism involving arm-chopping? To address this question, we generated an X0 HJ variant in which the opposing oligonucleotides X0-2 and X0-4 were modified to contain three hydrolysis-resistant phosphorothioate linkages (SP) between nucleotides 30, 31, 32 and 33 (Figure 3A). This renders these strands more resistant to cleavage by both Yen1 and GEN1 (Figure 3B) and favours the processing of this HJ by symmetrical resolution, i.e., by the introduction of two nicks on oligos X0-1 and X0-3, respectively. We compared the ability of both resolvases to process this structure with respect to an unmodified X0 HJ and verified that the ability of each enzyme to introduce a nick at nucleotide 31 in the oligo X0-1 was similar for both substrates (Figure 3C). Remarkably, when analysing the same reactions on native gels, we observed that both the RF-like and small duplex products that Yen1 generates on the X0 HJ disappear when the X0-2SP is employed, while most of the nicked duplex product remained (Figure 3D). We quantified the formation of nicked duplex and total cleavage (RF-like + nicked duplex + small duplex) in each reaction and observed that, for GEN1, total cleavage is equivalent to nicked duplex formation, as expected for a canonical resolvase. For Yen1, the nicked duplex represents ∼2/3 of the total cleavage (19% vs 28%) on a normal X0 HJ, with an undetermined contribution from each mechanism. However, on the X0-2SP virtually all cleavage products correspond to the nicked duplex (14%), which in this case can only arise from symmetrical resolution (Figure 3D). Therefore, these results demonstrate that Yen1 is capable of symmetrical resolution of an intact HJ, despite being endowed with an alternative arm-chopping mode of HJ processing.

Yen1 and GEN1 display a different preference in strand cleavage on a HJ with a fixed conformation

In the presence of Mg^{2+}, HJs undergo a conformational change from an open, square structure into a form where pairs of arms are coaxially stacked (92). This implies the existence of two DNA strands that will appear as continuous as opposed to two exchanging strands. Some HJ resolvases like RuvC, T7 Endo I and GEN1 show a preference for the cleavage of the continuous strands (34,56,93,94), while Hjc or T4 Endo VII incise the exchanging strands (95–97). To assess if Yen1 displays any bias in cleavage orientation, we determined the incision sites it produced on a J3 synthetic HJ, which in solution exists almost exclusively as a conformer with arm-stacking of 2 over 4 and 1 over 3 (Figure 4A) (33). While GEN1 preferentially nicked the J3 HJ in the *x* and *h* strands (Figure 4B–D), as previously reported (56) and similarly to CtGEN1 (48), Yen1 introduced incisions mostly in *b* and *r* strands (Figure 4B–D). These results indicate that, like other GEN1-family resolvases, Yen1 also

Downloaded from https://academic.oup.com/nar/article/50/1/259/6470689 by Irene Ruiz user on 01 July 2022

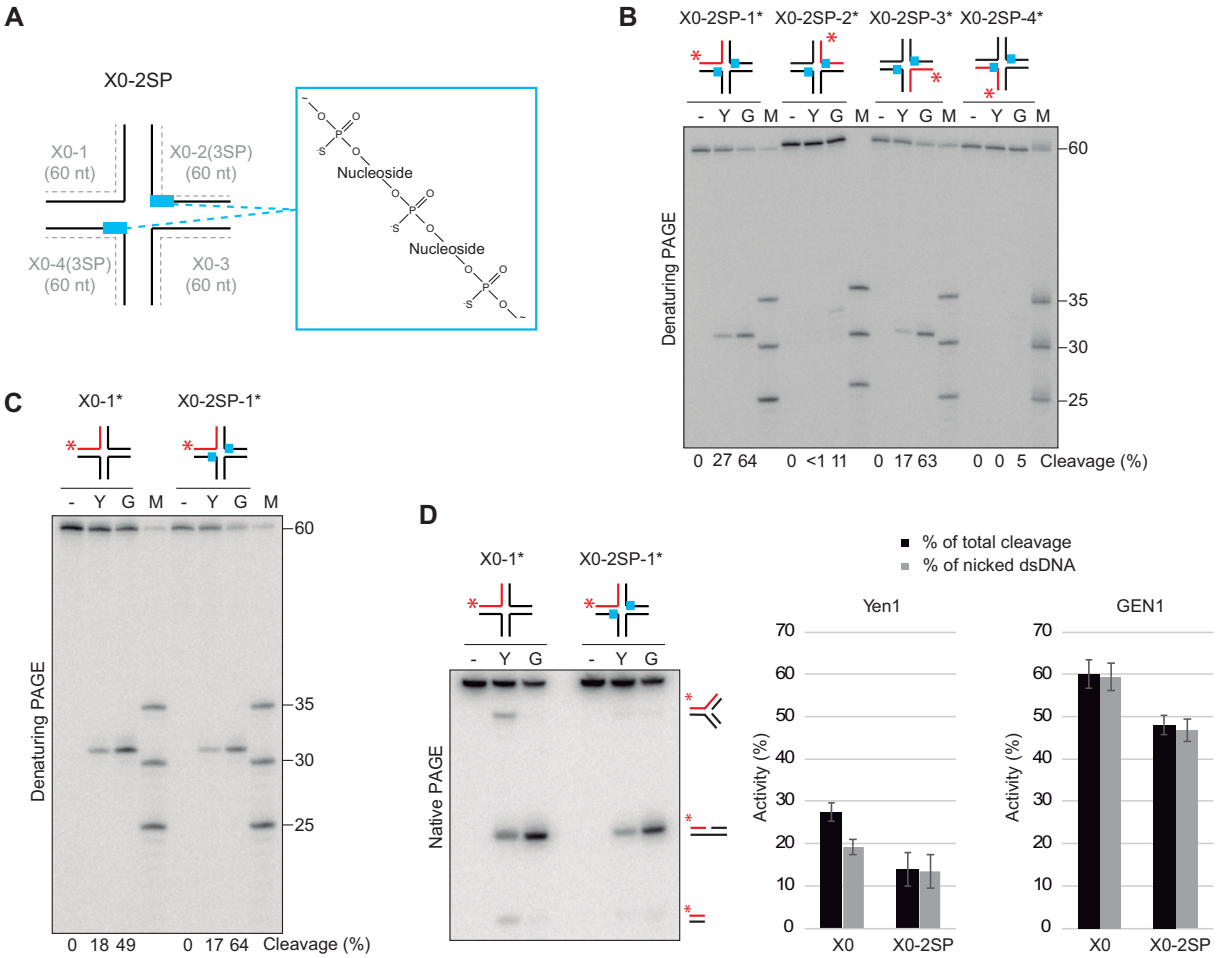

Figure 3. Yen1 can resolve HJs symmetrically. (**A**) Scheme of the SP-containing X0 HJ employed in the assay (X0-2SP), which contains 3 hydrolysis-resistant phosphorothioate linkages between nucleotides 30, 31, 32 and 33 of oligos X0-2 and X0-4 (indicated by a blue box). (**B**) Reactions were carried out and labelled essentially as in Figure 1, using 5 nM X0-2SP, 5′-^{32}P-end-labelled (asterisk) and 5 nM Yen1$^{\lambda}$ (30 min, 30°C) or GEN1$^{1\text{-}527}$ (2.5 min, 37°C). Reaction products were analysed by 10% denaturing PAGE followed by phosphorimaging and quantified using ImageQuant. (**C**) Reactions with X0 or X0-2SP (5 nM) 5′-^{32}P-labelled in X0-1 were incubated with Yen1$^{\lambda}$ or GEN1$^{1\text{-}527}$ in the same conditions as in (B) and analysed by 10% denaturing PAGE. (**D**) The same reactions as in (C) were analysed by 10% native PAGE (left panel). A representative gel is shown. The formation of nicked dsDNA products and the total amount of all cleavage products were quantified (right panel). Data represented as mean values ± SD ($n = 3$).

displays a strong bias for the cleavage of one particular axis of the J3, but in this case preferring the opposite one.

A novel 5′-3′ exonuclease activity in Yen1 prevents the ligation of its HJ resolution products

GEN1 was first characterized as a canonical HJ resolvase due to its ability to introduce symmetrical cuts across the junction, leading to the formation of nicked dsDNA molecules that can be ligated without any further processing (10). As we have shown, Yen1 can also introduce symmetrical incisions, but its ability to produce resolution products that can be directly ligated remains unaddressed. Therefore, we decided to test if HJ resolution by Yen1 also fulfils this condition. For this purpose, we employed the X1-T asymmetrical HJ, which allows the detection of ligation products after resolution (40). Resolution of X1-T HJ across strands X1-1T (53 nt, 5′-labelled) and X1–3 (60 nt) and further re-ligation of the nicked product with T4 DNA ligase creates a new hybrid 5′-labelled strand of 60 nt that can be detected by denaturing PAGE (Figure 5A). Using this set-up, we confirmed that GEN1 resolution products can be readily ligated (>40%) (Figure 5B), as previously reported (10,40,56). However, ligation products were almost undetectable for Yen1. Given that the nicks produced on this junction are symmetrical and thus *a priori* able to be sealed, we speculated that Yen1 might be further processing its cleavage products. To test this hypothesis, we created nicked dsDNA substrates and determined whether Yen1 could act on them. When we labelled the 5′-phosphate group at the nick, we observed that incubation with Yen1 resulted in the loss of the labelling, as determined by the appearance of a fast-migrating band in both native and denaturing gels (Figure 5C, left panel). Conversely, when labelling the 3′-end of the same strand downstream the nick, Yen1 produced a slight shift of the substrate in native PAGE and the degradation of the substrate up to 3 nucleotides in denaturing PAGE (Figure 5C, right panel). Both results suggest that Yen1 is endowed with a 5′-3′ exonuclease activity specific for nicked DNA molecules. To further characterize this pre-

Downloaded from https://academic.oup.com/nar/article/50/1/259/6470689 by Irene Ruiz user on 01 July 2022

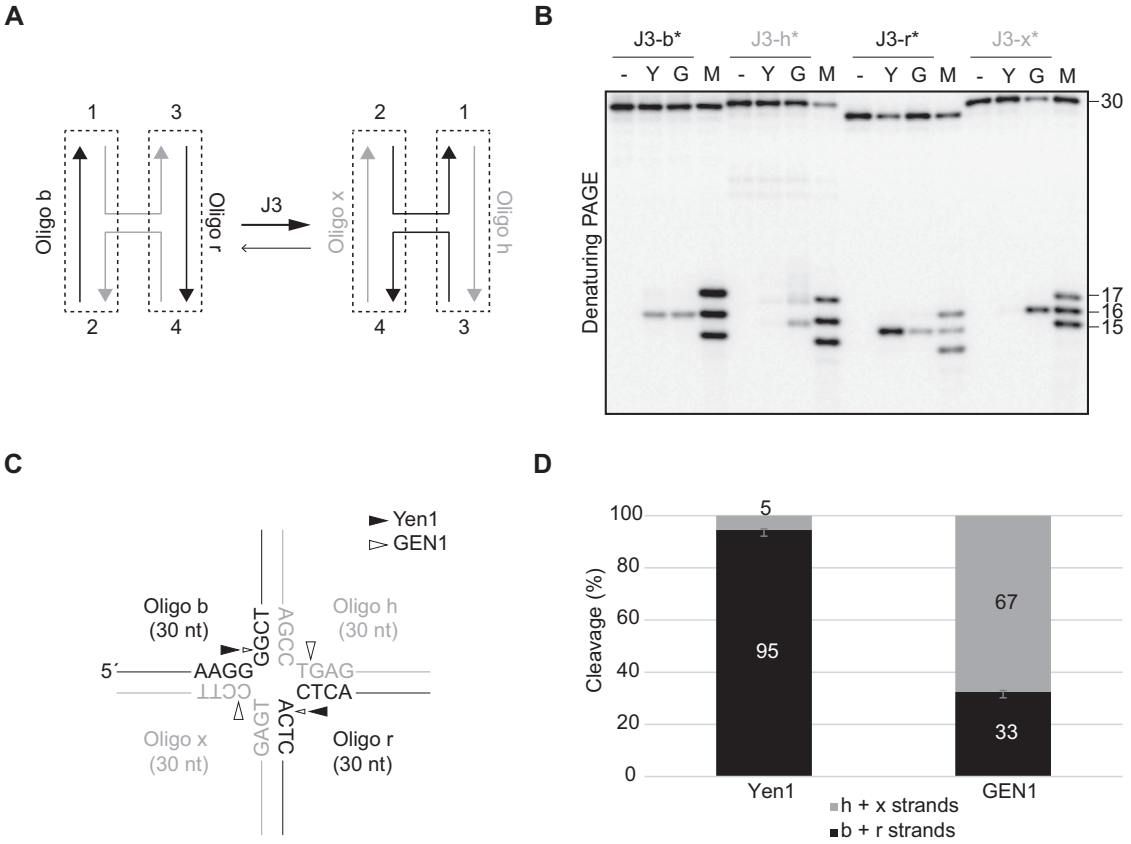

Figure 4. Yen1 shows a bias for axis cleavage of the J3 HJ. (**A**) Representation of the stacking conformers of the unbound J3 HJ substrate in solution. In its predominant state, oligos *x* and *h* (grey) behave as continuous strands while *b* and *r* (black) are crossing strands. (**B**) 5 nM J3 HJ 5′-^{32}P-labelled on the indicated strands was incubated with 50 nM Yen1$^{\lambda}$ (30°C, 5 min) or 5 nM GEN1 (37°C, 5 min). (–) control reaction without enzyme. Reaction products were analysed by 10% denaturing PAGE followed by phosphorimaging and quantified using ImageQuant. A representative gel is shown. A mixture of 5′-^{32}P-end-labelled oligos of defined length (15, 16, 17 and 30 nt) were used as markers (M). (**C**) Schematic representation of the main cleavage sites; arrow size indicates preferential cleavage on the J3 HJ by Yen1 (black arrows) and GEN1 (white arrows). (**D**) Quantification of the proportion of the cleavage of *h* + *x* strand versus *b* + *r* strands from (B). Data represented as mean values ± SD ($n = 3$).

viously undescribed exonuclease activity, we created a series of 3′-labelled dsDNA substrates with gaps of increasing length and checked if Yen1 could extend such gaps (Figure 5D). We observed that nicks and gaps up to 2 nt could be efficiently extended into 3-nt gaps. However, 3-nt gaps became poor substrates for Yen1 exonuclease activity and 4- or 5- nt gaps were not further extended. A possible effect of DNA breathing at the nick followed by endonucleolytic cleavage of the resulting pseudo-flap was ruled out by comparing the processing of the nicked dsDNA and 5′-flap substrates at different temperatures, with no obvious stimulation of the exonuclease activity at higher temperatures (Supplementary Figure S6A). Importantly, the inclusion of an SP linkage between the first two nucleotides of the downstream oligo in a nicked dsDNA substrate prevented Yen1 from further processing the nicked dsDNA (Figures 5E and Supplementary Figure S6B). The same experiment revealed that GEN1 is also endowed with this exonuclease activity, albeit comparatively weaker and excising only 1 nt (Figure 5E). On the other hand, neither Yen1 nor GEN1 display exonuclease activity on the preferred substrate for Rad2/XPG-family 5′-3′ exonucleases, a 5′-recessed dsDNA substrate (Supplementary Figure S6C). Finally, we hypothesized that if this previously undetected exonuclease activity was processing the resolution products of Yen1 on the X1-T HJ and preventing their ligation, the inclusion of a SP linkage between nt 31–32 in the oligo X1-3 of this X1-T HJ (1 nt at the 3′of the incision for resolution) should prevent this activity and allow their ligation. Indeed, when the resolution products created by Yen1 on such X1-T-SP were incubated with T4 DNA ligase, the 60 nt ligated strand could be detected, unlike with the unmodified X1-T HJ (Figure 5F). Altogether, these results reveal the existence of a 5′-3′ exonuclease activity in Yen1 that specifically extends nicks in dsDNA molecules into single-stranded gaps up to 3 nt long. Such activity efficiently processes the products of symmetrical resolution by Yen1, rendering them unable to be ligated *in vitro*.

Yen1 can process plasmid-borne cruciform structures by both resolution and arm-chopping

In bacteria and archaea, the dimeric nature of resolvases facilitates the acceleration of second-strand cleavage to introduce near-simultaneous nicks across one of the axes of the HJ and ensure coordinated resolution (43,98). However,

Downloaded from https://academic.oup.com/nar/article/50/1/259/6470689 by Irene Ruiz user on 01 July 2022

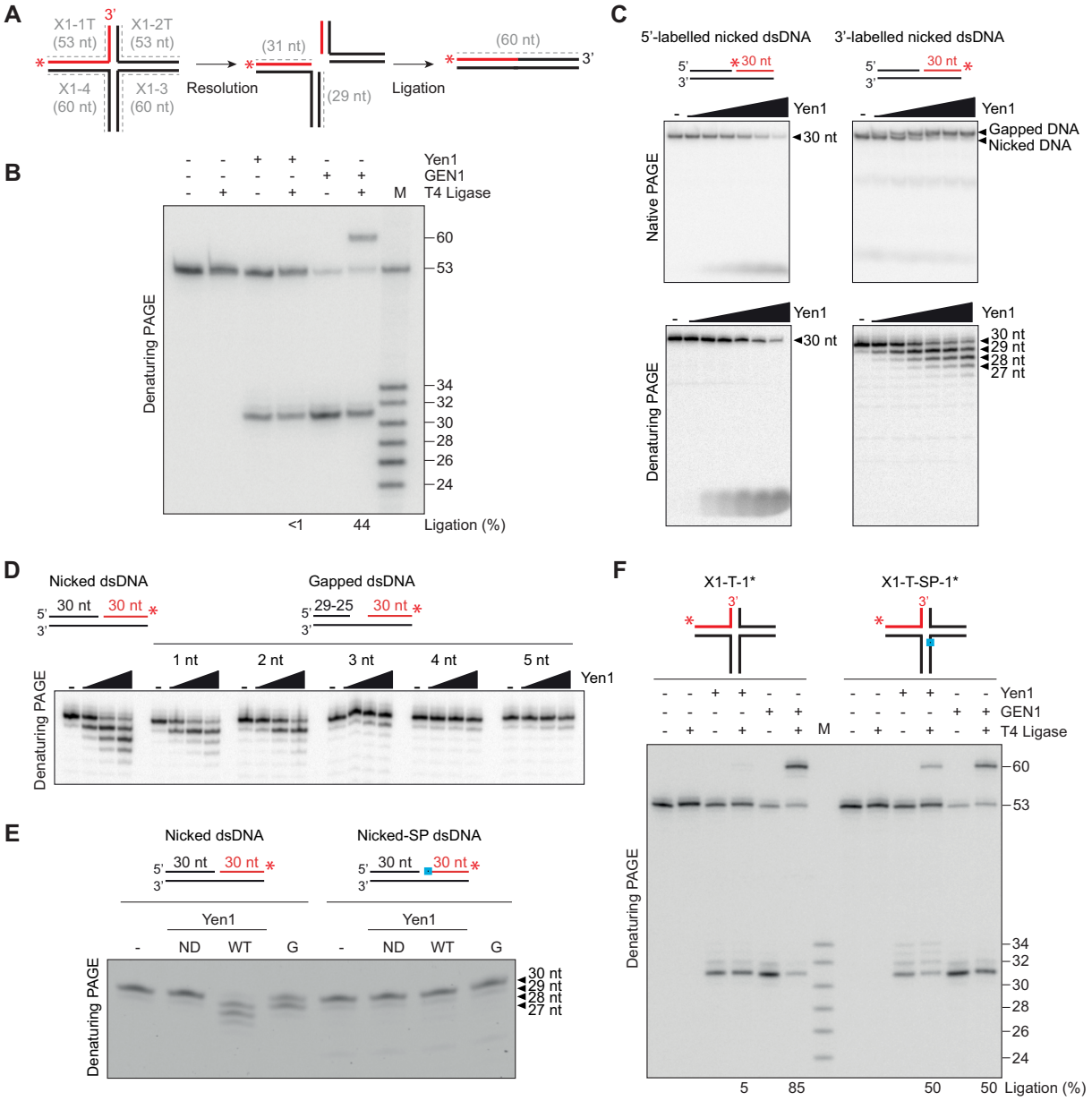

Figure 5. A 5′-3′ nick-specific exonuclease activity in Yen1 prevents the re-ligation of its resolution products. (**A**) Scheme of the re-ligation experiment employing the asymmetrical X1-T HJ substrate. Symmetric cleavage of this substrate, which contains a 53 nt, 5′-labelled (asterisk) oligo (red), and its subsequent ligation generates a new 60-nt labelled strand. (**B**) ∼0.5 nM X1-T HJ was incubated with 10 nM Yen1 or GEN1 for 30 min at 30°C or 37°C, respectively. (–) indicates no enzyme. Reactions were then supplemented with ligation buffer and T4 DNA ligase (5 U) and incubated for 1 h at RT. Products were analysed by 10% denaturing PAGE followed by phosphorimaging and quantified using ImageQuant. A mixture of 5′-^{32}P-end-labelled oligos of defined length (24, 26, 28, 30, 32, 34 and 53 nt) were used as markers (**M**). (**C**) ∼0.5 nM nicked dsDNA, either 5′-^{32}P-end (left panels) or 3′-^{32}P-end (right panels) labelled was incubated with increasing concentrations of Yen1$^{\lambda}$ (0, 0.25, 0.5, 1, 2, 4, 8 nM) for 10 min at 30°C. Products were then analysed by 10% native (top panels) or denaturing (bottom panels) PAGE and phosphorimaging. (**D**) ∼0.5 nM 3′-^{32}P-labelled dsDNA substrates with gaps of increasing length were incubated with increasing concentrations of Yen1 (0, 0.5, 2, 8 nM) for 10 min at 30°C. Products were analysed as in (C). (**E**) 10 nM nicked dsDNA or exonuclease-resistant (SP-linkage in the 5′ nucleotide, in blue) nicked dsDNA, 3′-6FAM-end-labelled (asterisk) on the indicated strand (red) were incubated with Yen1ND, Yen1$^{\lambda}$ and GEN1 (10 nM) for 10 min at 30°C or 37°C, respectively. (-) indicates no enzyme. Fluorescent products were analysed by 13% denaturing PAGE and scanned at 488 nm in a Typhoon FLA 9500. (**F**) As in (B), but employing both the unmodified X1-T HJ substrate and an X1-T variant containing a SP linkage between positions 31 and 32 of oligo X1–3 (X1-T-SP).

Downloaded from https://academic.oup.com/nar/article/50/1/259/6470689 by Irene Ruiz user on 01 July 2022

Yen1 orthologs are monomers in solution, like all the members of the Rad2/XPG family and, hence, it has been proposed that coordinated incisions require their dimerization on the HJs (40,48,53,56). After confirming that Yen1 is also a monomer in solution (Supplementary Figure S7), we employed plasmid-based substrates that extrude palindromic sequences as a cruciform, like pIRbke8 derivatives (56,99) or pIR9 (47) to assess if Yen1 was able to introduce pair of nicks in a coordinated manner, this is, within the lifetime of the enzyme dimer–HJ complex. Coordinated cleavage of the cruciform structure leads to the linearization of the plasmid, while individual nicks on the cruciform allow the release of negative supercoils and result in the reabsorption of the cruciform into a relaxed nicked circular DNA (Figure 6A, upper and lower row). It has been shown that dimers of Rad2/XPG-family resolvases introduce coordinated nicks on the cruciform within the lifetime of the enzyme-DNA complex, leading mainly to the formation of linear products (40,47,48,56). To test if Yen1 also displays a similar level of coordination when processing this type of substrates, we incubated the cruciform-containing plasmid pIR9 with either the phosphorylated or lambda phosphatase-treated version of Yen1 and a mixture of products was observed in both cases (Figure 6B). Phosphorylated Yen1 converted most of the plasmid into its low-mobility, relaxed circular form, whereas the major product after incubation with the more active, dephosphorylated version of Yen1 was the linear form (Figure 6B). These results suggest that the activation of Yen1, in addition to the enhancement of its nuclease activity, may also improve its ability to carry out coordinated cleavage within the lifetime of the enzyme dimer-DNA complex.

However, we were still surprised by the level of non-coordinated cleavage that Yen1 was able to promote, as evidenced by the presence of the relaxed form of the plasmid in these experiments. Given our previous observations of Yen1 arm-chopping activity, we wondered whether this activity could also act on a cruciform-bearing plasmid. If so, it would imply a coordinated pair on incisions, but in an asymmetrical manner, that could lead to the formation of a relaxed, gapped circle (Figure 6A, central row), a product that would be electrophoretically indistinguishable from a relaxed, nicked circle in an agarose gel. To elucidate if Yen1 gives rise to nicked circles (uncoordinated cleavage) and/or gapped circles (coordinated cleavage), we designed two different experiments. First, we argued that if the relaxed circles were nicked molecules, they could be re-ligated; if they contained ssDNA gaps, they should not re-ligate. As shown in Figure 6C, nicked circles produced with Nt.BspQI are readily ligated, and migrate as a supercoiled DNA band, while only a minor fraction of the relaxed circle can re-ligate in the reactions with Yen1. This suggests that the main circular product generated by Yen1 could be a gapped molecule. However, it is important to consider that Yen1 could also produce a relaxed circle that cannot be re-ligated if the nicking of a single strand is followed by its exonuclease activity. Indeed, Nt.BspQI-nicked pIR9 cannot be re-ligated upon treatment with Yen1 (Figure 6D). Therefore, a second experiment was designed to specifically detect the DNA fragment that would be released only if Yen1 catalysed an arm-chopping reaction on one of the hairpins of the cruciform structure (Figure 6E), by labelling all the reaction products and analysing them in a denaturing gel. For this experiment, the cruciform-based plasmid was incubated with Yen1$^{\lambda}$, Yen1$^{ON\text{-}\lambda}$ (a phosphatase-treated version of Yen1^{ON}, see below), Yen1ND, GEN1 as a control for a linear product, Nt.BspQI as a control for a nicked product, and EcoRI, which is commonly used to test the extrusion level of the plasmid. When these reactions were analysed in a denaturing gel, we could only detect bands consistent with the expected size of the released hairpin (66 nt) in those containing active Yen1, but not in any of the other controls (Figure 6F). All these results strongly suggest that a significant fraction of the relaxed, circular molecules arise from an arm-chopping mechanism. Therefore, Yen1 seems to mainly promote the coordinated incision of plasmid-borne cruciform structures, albeit occasionally in an asymmetrical manner.

The assembly of a Yen1 dimer on the HJ accelerates the rate of the first incision during HJ resolution

Our results with the plasmid-borne cruciform indicate that HJ processing by Yen1 proceeds mostly by the introduction of coordinated incisions within the lifetime of a nuclease dimer-HJ complex. For the dimeric prokaryotic and mitochondrial resolvases, such coordination is ensured by the acceleration of the cleavage of the second strand after the first incision (98). However, eukaryotic Rad2/XPG family HJ resolvases are monomeric in solution and dimerization happens on the HJ (40,47,48,53). It has been shown for human GEN1 that dimerization on the HJ substrate stimulates the first incision of the junction by one of the monomers, which is the rate-limiting step for HJ resolution (40), while experiments with CtGEN1 have confirmed that cleavage of the second strand is accelerated after the first incision (48,100). To test if the formation of the dimer on a HJ could also favour the initial incision by Yen1, we created a modified X0 HJ with a SP bond at the expected cleavage position of Yen1 in oligo X0-3, between nucleotides 31 and 32 (Figure 7A). When incubated with Yen1 or GEN1, this X0-SP cannot be resolved as efficiently as a normal X0 HJ junction, mostly due to a drastic decrease in the cleavage of strand X0-3 (Figure 7B and C), as previously shown for GEN1 (40). Then, we titrated catalytically inactive Yen1ND, which is still binding-proficient (see Materials and Methods: 'Bio-layer interferometry assays'), in reactions with limiting amounts of active Yen1 to measure how an increase of total dimers in the reaction would affect the initial incision. This experiment was performed both with lambda phosphatase-treated (Figure 7D-F) and phosphorylated (Supplementary Figure S8A and B) versions of Yen1 and Yen1ND. In agreement with published results for GEN1 (40), the nicking of strand X0-1 was stimulated by addition of Yen1ND, up to a 1:16 WT:ND molar ratio (Figures 7D, E, Supplementary Figure S8A and B). As expected, further titration resulted in an inhibitory effect, likely due to the sequestration of HJs by inactive dimers. A kinetic analysis of the nicking of the X0-1 oligonucleotide in denaturing gels confirmed a 2-fold increase in the observed reaction rate when comparing Yen1 alone or with a 16-molar excess of inactive enzyme (Figure 7F). These results indicate that formation of a Yen1 dimer on the HJ favours the rate-limiting, initial incision.

Downloaded from https://academic.oup.com/nar/article/50/1/259/6470689 by Irene Ruiz user on 01 July 2022

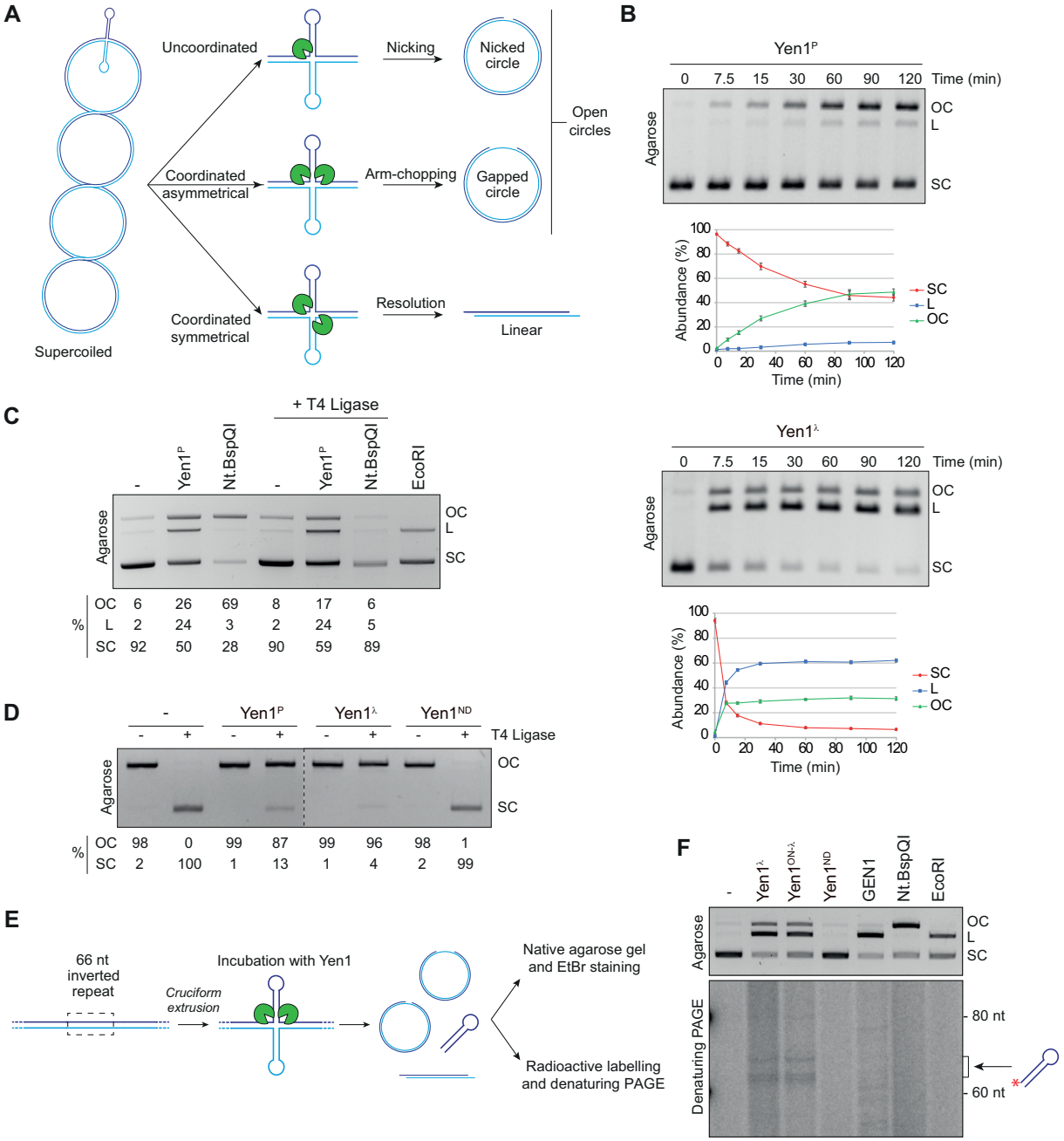

Figure 6. Yen1 processes plasmid-borne cruciform structures by coordinated incisions. (**A**) Schematic representation of the cruciform cleavage assay used to determine whether incisions are coordinated or not. A third possibility incorporating arm-chopping (central pathway) is added to the two classical outcomes of the assay. (**B**) 4.5 nM pIR9 plasmid was incubated with 90 nM $Yen1^{P}$ or $Yen1^{\lambda}$ at 30°C the indicated times. Products were analysed in ethidium bromide-post-stained 0.8% agarose gels. Analysis and quantification were carried out with Image Lab software (Bio-Rad). A representative gel is shown for each enzyme. Data represented as mean values ± SD ($n = 3$). OC: open circle; L: linear; SC: supercoiled. (**C**) Ligation experiment with pIR9. 4.5 nM pIR9 was incubated with 90 nM $Yen1^{P}$ or 10 U Nt.BspQI for 1 h at 30°C or 50°C, respectively. Products were then purified, treated with T4 DNA ligase for 1 h at 37°C, and then analysed and quantified as in (B). EcoRI was used as a control of the extrusion level of the plasmid. (**D**) Ligation experiment with pre-nicked pIR9. 4.5 nM nicked pIR9 (see Materials and Methods) was either mock-treated (–) or incubated with 90 nM $Yen1^{P}$, $Yen1^{\lambda}$ or $Yen1^{ND}$ for 90 min at 30°C. Then it was purified, ligated and analysed as in **(C)**. Dotted lines indicate splicing of superfluous lanes. (**E**) Schematic of the experimental set-up to detect the hairpins released by arm-chopping on pIR9. (**F**) 4.5 nM pIR9 was incubated with 90 nM Yen1 ($Yen1^{\lambda}$, $Yen1^{ON\text{-}\lambda}$ or $Yen1^{ND}$), 50 nM GEN1, 10 U Nt.BspQI or 1 U EcoRI for 90 min. Then, reactions were treated with 1 U thermosensitive alkaline phosphatase (FastAP) for 1 h at 37°C and inactivated for 5 min at 75°C. Half of the reaction was loaded on a 0.8% agarose gel (upper panel) and visualised with ethidium bromide post-staining. The other half was denatured, labelled with T4 PNK and ^{32}P-γ-ATP and analysed by 15% denaturing PAGE and phosphorimaging. (–) indicates no enzyme. The arrow indicates products of expected sizes.

Downloaded from https://academic.oup.com/nar/article/50/1/259/6470689 by Irene Ruiz user on 01 July 2022

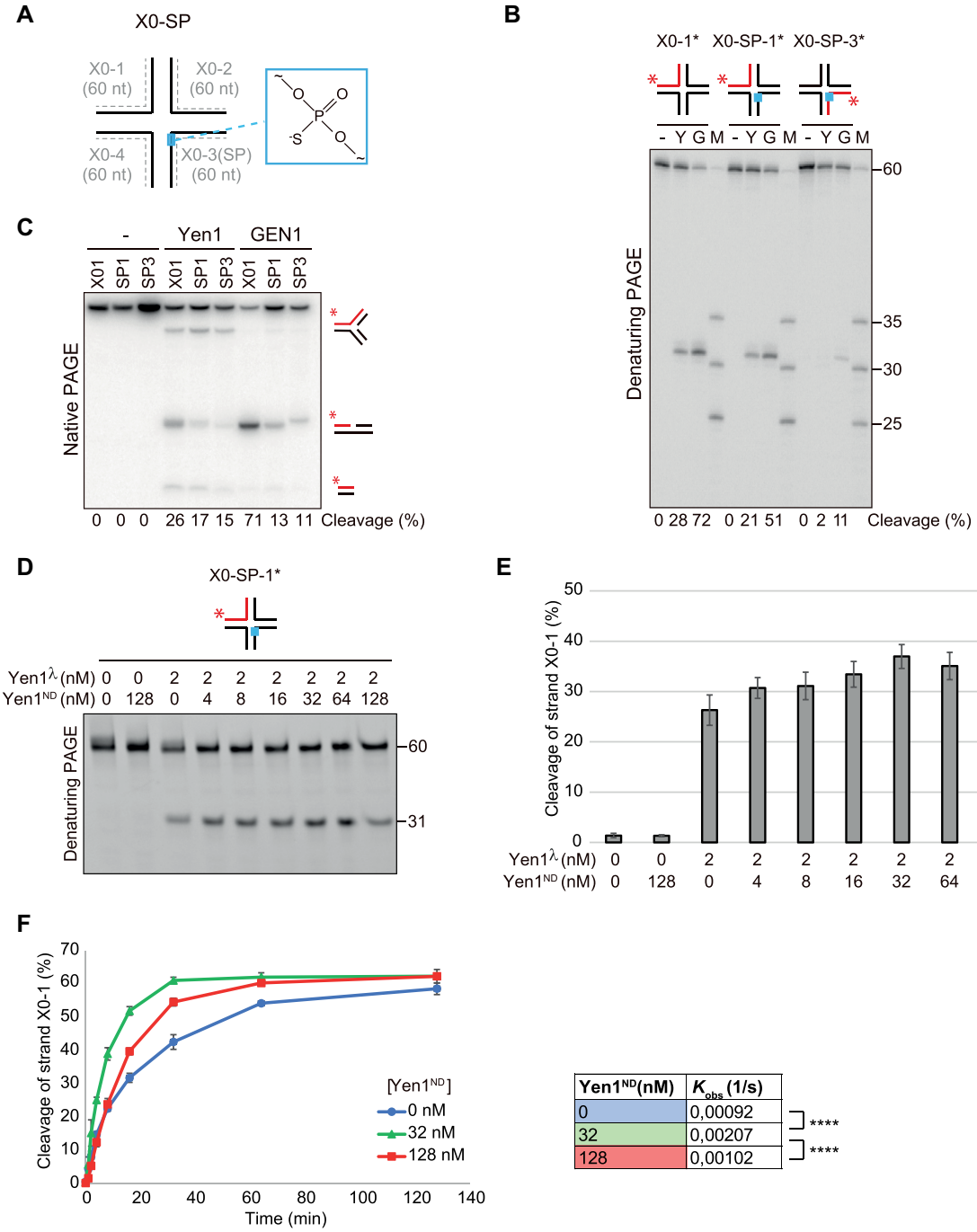

Figure 7. Yen1 dimerization on the substrate favours its first incision. (**A**) Schematic representation of a modified X0 HJ with a phosphorothioate linkage (in blue) between positions 31–32 nt of oligo X0-3 (X0-SP). (**B**) 5 nM unmodified X0 5′-^{32}P-end-labelled in oligo X0-1 and X0-SP 5′-^{32}P-end-labelled in oligonucleotide X0-1 or X0-3 were incubated with 5 nM Yen1$^{\lambda}$ for 5 min at 30°C or 5 nM GEN1$^{1\text{-}527}$ for 2.5 min at 37°C. Asterisk indicates labelled position and labelled strand is indicated in red. (–) indicates control reaction with no enzyme. Products were analysed by 10% denaturing PAGE. Cleavage was quantified as shown. 5′-^{32}P-end-labelled oligos of defined length (25, 30, 35 and 60 nt) were used as markers (M). (**C**) Same reactions as in (B) were analysed by 10% native PAGE. Possible reaction products are indicated on the right. (**D**) 10 nM 5′-6FAM-HJ-X0-SP was incubated with 2 nM Yen1$^{\lambda}$ and the indicated concentrations of Yen1ND for 5 min at 30°C. Products were analysed by 10% denaturing PAGE and scanned at 488 nm in a Typhoon FLA 9500. A representative gel is shown. (**E**) Quantification by ImageQuant of the reaction shown in (D). Data represented as mean values ± SD ($n = 3$). (**F**) Kinetic analysis of nicking on strand X0-1 of 10 nM 5′-6FAM-HJ-X0-SP by 2 nM Yen1$^{\lambda}$ pre-mixed with 0, 32 or 128 nM Yen1ND. Aliquots were removed at different times (0, 1, 2, 4, 8, 16, 32, 64 and 128 min) and reaction products were resolved, visualised and quantified as in (D, E). Data represented as mean values ± SD ($n = 3$). Reaction progress was fitted to a single exponential function (see Materials and Methods) to estimate the observed reaction rates (K_{obs}); ****, $P < 0.0001$ (F-test).

Downloaded from https://academic.oup.com/nar/article/50/1/259/6470689 by Irene Ruiz user on 01 July 2022

Yen1^{ON} displays the same cleavage specificity as Yen1

Yen1^{ON} is a mutant version of Yen1 where all nine serines in CDK consensus sites (Figure 1A) have been substituted for alanines, rendering the protein constitutively active and nuclear throughout the cell cycle (69). This mutant serves as a powerful tool to explore the consequences of its premature activation without the need of interfering with the cell cycle progression machinery (68,69,73–80). While we have previously shown that the range of substrates that Yen1^{ON} can process overlaps entirely with that of Yen1 (69,70), we did not know whether the specificity of the incisions within each substrate remained unaltered, so we mapped the cleavage sites produced by Yen1^{ON} on the same set of substrates (Supplementary Figure S9A). We did not observe any difference on the position of the sites cleaved by Yen1^{ON} with respect to those cleaved by the wild-type enzyme, confirming that despite its lack of CDK-dependent regulation, Yen1^{ON} retains the same cleavage specificity, thus representing a good proxy for the status of maximum Yen1 activation. However, when comparing the kinetics of *in vitro*-dephosphorylated wild-type Yen1 with those of Yen1^{ON}, we noticed that the cleavage rate of the former was always lower (Supplementary Figure S9B and C). In this sense, previous phosphomapping analyses of Yen1 revealed that there are at least 20 S/T residues at non-CDK consensus sites phosphorylated *in vivo* (69,70,101). Since the Yen1^{ON} preps we employed were not *in vitro*- dephosphorylated, we wanted to assess if phosphorylation at those non-CDK consensus sites could also be contributing to the regulation of Yen1 activity. For this, we dephosphorylated Yen1^{ON} by treatment with lambda phosphatase and compared its ability to process different substrates with respect to the mock-treated protein (Supplementary Figure S9D and E). Both versions displayed similar cleavage kinetics, indicating that phosphorylation at CDK sites represent the major regulatory switch for Yen1 nuclease activity, with none or minor contribution from other phosphoresidues. Since this result did not explain the differences in activity between dephosphorylated Yen1 and Yen1^{ON}, we tested if some level of residual phosphorylation could still be detected for these proteins after lambda phosphatase treatment using Phos-Tag containing SDS-PAGE gels that specifically reduce the mobility of phosphoproteins. Indeed, we observed that while the phosphatase treatment apparently abolished all phosphorylation on Yen1^{ON}, a detectable shift was still present for wild-type Yen1 (Supplementary Figure S9F). Therefore, the most likely explanation for the difference in activity between dephosphorylated wild-type Yen1 and Yen1^{ON} is due to the inability of lambda phosphatase treatment to completely remove all phosphorylation from relevant serines at Yen1 CDK consensus sites and thus preventing full activation of the enzyme.

Expression in yeast of constitutively nuclear human GEN1 does not fully recapitulate the genotoxicity of misregulated Yen1

The ability of both Yen1 and GEN1 to target branched DNA molecules is tightly controlled throughout the cell cycle. To understand the importance of such regulation, two mutants that can access and cleave their potential targets at any cell cycle stage—Yen1^{ON} and GEN1^{nuc}—were expressed in budding yeast and human cells, respectively (54,69). Interestingly, while expression of both these mutants leads to an increase of COs, only Yen1^{ON} causes hypersensitivity to genotoxic stress. To figure out whether this higher toxicity of Yen1^{ON} expression in yeast cells depends on some specific feature of the yeast chromatin biology or on the biochemical differences between Yen1 and GEN1, we decided to set up an *in vivo* experiment to compare the effects of expressing these mutants in the same organism. For this, we created a series of *S. cerevisiae* strains harboring different cassettes to express Yen1, Yen1^{ON}, GEN1, GEN1^{nuc} and the GEN1 truncated versions GEN1$^{1\text{-}527}$ and GEN1$^{1\text{-}527\ nuc}$, all under the control of either the inducible *GAL1* or the constitutive *GPD1* promoters in both wild-type and resolution-deficient (*mus81Δ yen1Δ*) backgrounds. To ensure that any observed toxicity for Yen1^{ON} was not merely due to a dose or localization effect, we aimed for a set of strains where GEN1 variants displayed constitutive nuclear localization as well as similar or higher protein expression levels and similar or higher biochemical activity in whole-cell extracts when compared to strains carrying Yen1^{ON}. Among all combinations tested, these premises could only be fulfilled in media containing galactose when Yen1 and Yen1^{ON} were expressed under the control of the *GPD1* promoter, and GEN1$^{1\text{-}527}$ and GEN1$^{1\text{-}527\ nuc}$ were expressed under the control of the *GAL1* promoter (Figure 8A–C). Under these conditions, we compared the effect of Yen1^{ON} and GEN1$^{1–527\ nuc}$ in increasing hypersensitivity to the genotoxic agent methyl methanesulfonate (MMS) in a wild-type background (Figure 8D). To verify the functionality of the enzymes, we also performed this experiment in the resolution-deficient *mus81Δ yen1Δ* double mutants (Figure 8E), where premature activation of Yen1 provides increased resistance to MMS (69). In the wild-type strain, expression of Yen1^{ON} conferred strong sensitivity at the lower dose of MMS tested (Figure 8D), whereas expression of GEN1$^{1–527\ nuc}$ induced a milder sensitivity, despite showing comparable expression levels and a more potent nuclease activity on extracts (Figure 8A and B). However, when we analysed the survival of the *mus81Δ yen1Δ* double mutants to the MMS treatment, we observed that Yen1^{ON} was also more efficient in providing resistance to MMS than GEN1$^{1–527\ nuc}$ (Figure 8E). Therefore, while Yen1^{ON} expression is more toxic than that of GEN1$^{1–527\ nuc}$, despite its lower biochemical activity in whole-cell extracts, we cannot conclusively affirm that this toxicity derives from specific differences in their biochemical properties, as GEN1$^{1–527\ nuc}$ does not seem comparably functional in the processing of HR intermediates when expressed in yeast.

DISCUSSION

The original identification of Yen1 as a canonical HJ resolvase in *S. cerevisiae* relied on experiments carried out employing whole-cell extracts and protein immobilized on agarose beads (10). Since then, much of what we know about Yen1 properties has been extrapolated from biochemical analyses of other orthologs in the subclass IV of the Rad2/XPG family. The biochemical characterization

Downloaded from https://academic.oup.com/nar/article/50/1/259/6470689 by Irene Ruiz user on 01 July 2022

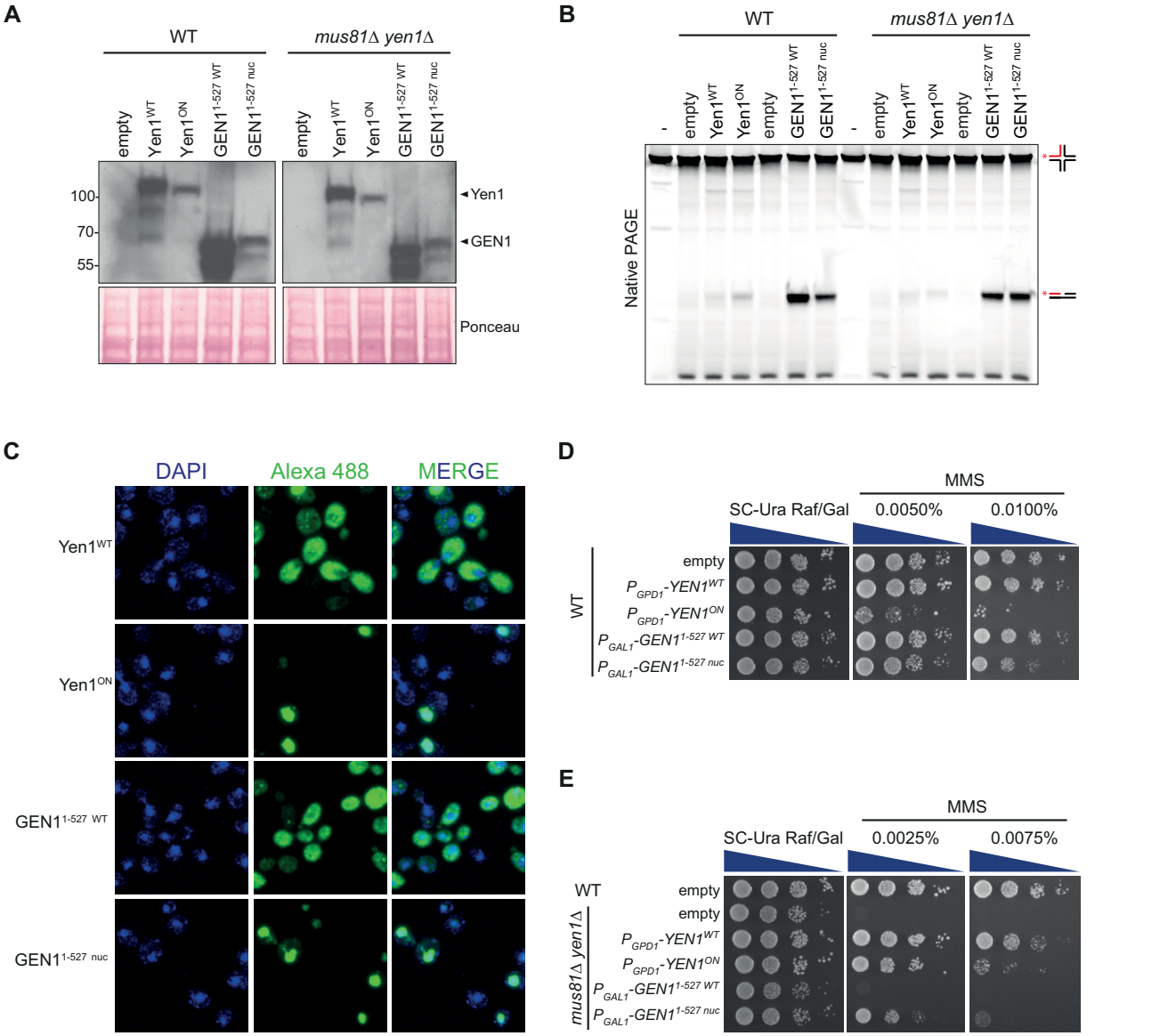

Figure 8. Expression of deregulated Yen1 and GEN1 mutants in *S. cerevisiae*. (**A**) Western-blot analysis of protein expression levels in soluble extracts from WT or *mus81Δ yen1Δ* strains transformed with the plasmids p416GPD1-YEN1$^{WT/ON}$-V5-6xHis or pYES-EXP52-GEN1$^{1–527\ WT/nuc}$-V5-6xHis growing in SC-URA containing 1% raffinose and 2% galactose. Proteins were detected with an α-V5 antibody and Ponceau staining was employed as a loading control. (**B**) Resolution assay employing soluble extracts from (A). 2 μg total protein were incubated with 50 nM IRDye-700 fluorescent X0 HJ for 1 h at 30°C. Products were analysed in 10% native PAGE and visualised in an Odyssey (LI-COR) infrared scanner. (**C**) Analysis of the subcellular localization of Yen1 and GEN1 variants by immunofluorescence employing α-V5 (1:200) as primary antibody and α-mouse Alexa 488 (1:200) as secondary antibody. DNA was stained with DAPI. (**D**) Wild-type strains carrying the indicated constructs were plated on media with increasing amounts of MMS, grown at 30°C for 72 h and photographed. (**E**) As in (D), but employing *mus81Δ yen1Δ* strains.

of Yen1 presented in this work confirms some of the predictions about its mode of HJ processing, but also reveals unanticipated properties of this resolvase.

The high- and low-activity versions of Yen1 display identical incision patterns

We had previously shown that the phosphorylation status of Yen1 does not affect the range of branched substrates it can target (69), which are similar to those described for GEN1 (10,40,56). Here, we have additionally confirmed that these changes in phosphorylation do not alter the position of the incisions that Yen1 produces on a wide range of substrates (Figures 1, Supplementary Figures S3 and S4). In a similar way, the constitutively active mutant Yen1^{ON} incises all the tested substrates at identical positions when compared to the wild-type Yen1 (Supplementary Figure S9). Therefore, this work further substantiates that the activation of Yen1 by dephosphorylation does not qualitatively change how the enzyme processes these oligonucleotide-based substrates. The slightly lower activity observed with Yen1$^{\lambda}$ when compared to Yen1^{ON} derives from the inabil-

Downloaded from https://academic.oup.com/nar/article/50/1/259/6470689 by Irene Ruiz user on 01 July 2022

ity of lambda phosphatase to fully dephosphorylate Yen1 *in vitro*. These results suggest that some of the serines at CDK sites might become sterically occluded after phosphorylation due to a subsequent conformational change, rendering them less accessible to phosphatase treatment.

Yen1 may present a particular interaction mode with HJs and other substrates

Our analyses show that Yen1 and GEN1 cleave most oligonucleotide-based substrates at identical positions. However, overt differences were observed, not only regarding the unexpected arm-chopping and nick-exonuclease activities, but also in their preference for strand cleavage when employing the J3 HJ (Figure 4). Despite its closer phylogenetic relation to Yen1, fungal CtGEN1 presents a similar axis preference to human GEN1 (48), which suggests that Yen1 might dock on the junction or remodel it in a slightly different manner compared to GEN1 or CtGEN1 and, potentially, other orthologs. Such alternative preference could also arise from specific sequence requirements for Yen1 that differ from its orthologs. Interestingly, sequence alignments of its XPG-N nuclease domain show an insertion of more than 30 amino acids with respect to CtGEN1 and GEN1 in the region corresponding to their helical wedge (50,52) (Supplementary Figure S10). This insertion is predicted to be disordered and could modify the C-terminal part of the first of its α-helices (α2 in GEN1; α3 in CtGEN1) and/or increase considerably the size of the intervening coiled region. The helical wedge is important for the bending of the DNA substrate, containing several amino acids that establish direct contacts with the DNA bases and backbone and being located near conserved catalytic residues like D41 in Yen1 (D30 in GEN1, D38 in CtGEN1) (50,52). Thus, it could be envisaged that a different spatial configuration of this region could alter to some extent the binding of Yen1 (or the relative positioning of catalytic residues) with respect to its substrates, resulting in slightly different protein–DNA interactions when compared to its orthologs. Similarly, Yen1 chromodomain also displays notable differences with respect to GEN1 and CtGEN1, including a 6 amino acid insertion in its DNA interaction site and substitutions in most residues of its aromatic cage (50), which could have similar effects. Curiously, both the insertions in the predicted Yen1 helical wedge and chromodomain include five of the consensus CDK sites that are known to modulate Yen1 activity (Supplementary Figure S10) (69,70). In this sense, it would be interesting if future studies could determine whether some of Yen1 biochemical properties have evolved as a result of the inclusion of these regulatory regions within catalytic/DNA binding domains to enforce its strict cell cycle-dependent control.

We would also like to note that we have detected unanticipated cleavage products by human GEN1 on oligo X0-1 in substrates like the 3′-flap, splayed arm or ssDNA (Supplementary Figure S4). These products can be observed in GEN1 preparations from other groups (53). Since this activity can be observed on X0-1 as ssDNA, but not on ssDNA poly-T oligos, we think that this oligo may form a stable secondary structure that can be recognized and targeted by GEN1, but not Yen1, revealing another minor difference between the two enzymes.

Yen1 non-canonical activities and the paradigm of canonical HJ resolution

The paradigm of canonical resolution states that the symmetrical, coordinated incisions across one of the axis of the junction must occur within the lifetime of the enzyme-substrate complex, yielding nicked DNA molecules that can be sealed without the need for further processing (43,91). This work demonstrates that Yen1 can be considered a canonical resolvase since (i) it can create symmetrical cuts on a HJ (Figure 1), (ii) the incisions occur mainly in a coordinated manner (Figure 6) and (iii) its resolution products, in a first instance, could be ligated (Figure 5). However, the existence of the novel arm-chopping and nick-exonuclease activities plays a confounding role in the interpretation of biochemical assays traditionally employed to assess the coordination of incisions and the ligation of resolution products, respectively.

In this sense, our results regarding cleavage coordination with the cruciform extruding plasmid pIR9 (47) led us to propose an extension to the usual interpretation of this type of experiments. Thus, an undetermined, but likely major fraction of the relaxed circular species produced by Yen1 would correspond to gapped, rather than nicked circles, resulting from arm-chopping activity (Figures 6 and Supplementary Figure S5B). In this way, Yen1 would process this cruciform mainly in a coordinated, but not always symmetrical manner. This coordination would be consistent with the idea that Yen1, despite being a monomer in solution (Supplementary Figure S7), needs to dimerize on the substrate in order to accelerate the rate of the first incision (Figure 7D, F), the limiting step of the reaction, as previously proposed for other Rad2/XPG-family resolvases (47,48,50,52–54,56,102). It is important to highlight that the biochemical characteristics of Yen1 prevent a more quantitative approach in terms of establishing the kinetics of the two incisions created by the enzyme in the cruciform, akin to those performed with RuvC (41), Cce1 (42) or CtGEN1 (48). Some of the premises in these experiments cannot be met with Yen1, including the unequivocal adscription of the slowest migrating band to a single plasmid species or the direct relation between the generation of the linear product and the disappearance of the relaxed DNA molecules.

With respect to the nick-exonuclease activity, it is interesting to note that we have also detected it with GEN1, but it does not seem robust enough to prevent re-ligation of resolution products conspicuously (Figure 5E and F). Importantly, we have never observed this exonuclease activity of Yen1 on dsDNA, ssDNA (Supplementary Figure S4) or even a 5′-recessed dsDNA substrate (Supplementary Figure S6C) and it seems unlikely that it could stem from partial DNA breathing that creates pseudo-5′flaps at the nicks that could be processed endonucleolytically (Supplementary Figure S6A and B), reinforcing the notion that this activity is specific for nicked dsDNA molecules. Altogether, our results support that Yen1 has a canonical resolvase be-

Downloaded from https://academic.oup.com/nar/article/50/1/259/6470689 by Irene Ruiz user on 01 July 2022

haviour *in vitro*, despite the presence of two additional activities that may blur such classification.

Could the detrimental effects of Yen1 premature activation be due to non-canonical activities operating *in vivo*?

Yen1 and GEN1 ability to access and process their targets in chromatin is strictly regulated throughout the cell cycle (64,65,69–71). However, the misregulation of Yen1 seems to elicit a more detrimental effect than misregulation of GEN1, especially in terms of DNA damage sensitivity (54,69). Such effect could be explained either by Yen1 deregulation having more severe consequences due to its specific activities or by yeast system being generally more sensitive to misregulation of any nuclease. Our efforts to try to distinguish between these two possibilities have not allowed us to reach a definitive conclusion (Figure 8). Our experiments indicate that the expression in yeast of GEN1$^{1\text{-}527\ nuc}$ produces a milder phenotype than Yen1^{ON}, both in terms of hypersensitivity to MMS in wild-type cells and resistance to MMS in *mus81Δ yen1Δ* double mutants. Hence, if interpreted conservatively, these results would suggest that GEN1$^{1\text{-}527\ nuc}$ does not have a similar capacity to target branched DNA molecules to Yen1^{ON} in yeast, regardless of their physiological or pathological nature for the cell. Possible explanations for this could include that maximal HJ resolution activity *in vivo* requires additional Yen1-specific post-translational modifications or interactions that cannot occur with GEN1. Other groups have reported SUMOylation of Yen1, with important functions both in its targeting for degradation when bound to chromatin in G1 as well as in its potential to establish protein-protein interactions, although SUMOylation itself does not seem to modulate Yen1 biochemical activity (72,103). Also, a physical interaction between Yen1 and an uncharacterized protein coded by ORF YPL088W has been recently detected (80), but its significance remains unknown. At this stage, we cannot rule out that Yen1 may interact with proteins that target it to specific substrates *in vivo* nor that additional modifications may fine-tune control its biochemical activity.

Notwithstanding, it has been shown that expression of GEN1 can process repair intermediates and restore sporulation in *S. pombe mus81Δ* mutants (104). Moreover, the magnitude of the detrimental effect caused by Yen1^{ON} expression compared to GEN1$^{1\text{–}527\ nuc}$ in wild-type cells seems higher than the difference in their protective effect in *mus81Δ yen1Δ* strains (Figure 8D and E). Therefore, we could alternatively argue that, to some extent, Yen1 might present specific properties that lead to increased toxicity when prematurely activated compared to GEN1, specially taking into account the comparatively lower protein levels and overall HJ resolvase activity in whole cell extracts expressing Yen1^{ON} (Figure 8A and B). Whether this potential toxicity of Yen1 is due to the novel activities described in this work, or if they manifest *in vivo*, remains unclear. The nicked dsDNA-specific 5′-3′exonuclease activity described in this paper has been previously observed for other members of the Rad2/XPG family, like class II human FEN1 (105,106) and class III EXO1 (107), and, despite very weakly, also in the class IV DmGEN (55). In this sense, the low ligation efficiency observed for the resolution products of OsGEN-L, AtGEN1 and AtSEND1 (47,58) could arguably be due to the presence of a similar activity. With respect to Yen1 ability to excise one arm from a nicked HJ (*Ref-I* activity (47)) or an intact HJ (arm-chopping) (Figures 3, Supplementary Figures S3 and S5), at least one of these activities has also been described or can be observed in the experiments with the plant, fly and mammalian orthologs (47,53,58) (Figures 2 and Supplementary Figure S3), and hence seem rather widespread among the subclass IV of the Rad2/XPG family of nucleases. Despite this apparent conservation, it is not straightforward to envisage a possible biological role for an activity like the arm-chopping in the context of disengaging two DNA molecules connected by HJs, as it would inevitably lead to the generation of a DSB (Supplementary Figure S5B). Alternatively, it has been proposed that replication fork reversal, which leads to the formation of a HJ-like structure, may help stabilize stalled replisomes, sometimes leading to situations of transient over-replication (108). Then, template unwinding followed by flap processing or end-resection of the regressed arm would be required for its removal and replication termination. In this context, if such intermediates persisted until late stages of mitosis, the endonucleolytic processing of the regressed arm by arm-chopping could hypothetically provide an alternative way for its elimination. In the future, it would be interesting to take advantage of structural data to explore possible separation-of-function mutants that lack some of these non-canonical activities. With such tools in hand, we could ask if they play any functional role *in vivo*, like the processing of particularly adamant recombination or replication intermediates, or simply represent collateral consequences of the evolutionary adaptation of a monomeric SSE to perform a reaction that requires its dimerization and coordinated cleavage on a Holliday junction.

SUPPLEMENTARY DATA

Supplementary Data are available at NAR Online.

ACKNOWLEDGEMENTS

The authors would like to thank Gary Chan and Stephen C. West for various yeast strains, plasmids, and proteins; Daniela Kobbe for the pIR9 plasmid; Marina Guerrero-Puigdevall and Jordi Frigola for assistance with size exclusion chromatography; Marta Picado for technical assistance with fluorescence microscopy and Joao Matos, Jordi Frigola and Tomás Lama Díaz for constructive discussions and critical reading of the manuscript.

FUNDING

The Blanco lab was supported from MCIN / AEI / 10.13039/501100011033 [PID2020-115472GB-I00]; MCIN / AEI / 10.13039/501100011033 / FEDER ‘Una manera de hacer Europa’ [BFU2016-78121-P]; Xunta de Galicia (XdG) / FEDER ‘Una manera de hacer Europa’ [ED431F-2016/019, ED431B-2016/016 and ED431C 2019/013]; CIMUS receives financial support from the XdG / FEDER [ED431G 2019/02, Centro Singular de Investigación de

Downloaded from https://academic.oup.com/nar/article/50/1/259/6470689 by Irene Ruiz user on 01 July 2022

Galicia, accreditation 2019–2022]; F.J.A. and R.C. were recipients of pre-doctoral fellowships from XdG [ED481A-2015/011 and ED481A-2018/041]; V.H.-N. from MINECO and AEI [BES-2014-068734]. Funding for open access charge: Ministerio de Ciencia e Innovación and Agencia Estatal de Investigación [PID2020-115472GB-I00].
Conflict of interest statement. None declared.

REFERENCES

1. Wild,P. and Matos,J. (2016) Cell cycle control of DNA joint molecule resolution. *Curr. Opin. Cell Biol.*, **40**, 74–80.
2. Wu,L. and Hickson,I.D. (2003) The Bloom′s syndrome helicase suppresses crossing over during homologous recombination. *Nature*, **426**, 870–874.
3. Andersen,S.L., Bergstralh,D.T., Kohl,K.P., LaRocque,J.R., Moore,C.B. and Sekelsky,J. (2009) Drosophila MUS312 and the vertebrate ortholog BTBD12 interact with DNA structure-specific endonucleases in DNA repair and recombination. *Mol. Cell*, **35**, 128–135.
4. Boddy,M.N., Gaillard,P.H.L., McDonald,W.H., Shanahan,P., Yates,J.R. and Russell,P. (2001) Mus81-Eme1 are essential components of a Holliday junction resolvase. *Cell*, **107**, 537–548.
5. Castor,D., Nair,N., Déclais,A.-C., Lachaud,C., Toth,R., Macartney,T.J., Lilley,D.M.J., Arthur,J.S.C. and Rouse,J. (2013) Cooperative control of Holliday junction resolution and DNA repair by the SLX1 and MUS81-EME1 nucleases. *Mol. Cell*, **52**, 221–233.
6. Fekairi,S., Scaglione,S., Chahwan,C., Taylor,E.R., Tissier,A., Coulon,S., Dong,M.Q., Ruse,C., Yates,J.R., Russell,P. *et al.* (2009) Human SLX4 is a Holliday junction resolvase subunit that binds multiple DNA repair/recombination endonucleases. *Cell*, **138**, 78–89.
7. Fricke,W.M. and Brill,S.J. (2003) Slx1-Slx4 is a second structure-specific endonuclease functionally redundant with Sgs1-Top3. *Genes Dev.*, **17**, 1768–1778.
8. Garner,E., Kim,Y., Lach,F.P., Kottemann,M.C. and Smogorzewska,A. (2013) Human GEN1 and the SLX4-associated nucleases MUS81 and SLX1 are essential for the resolution of replication-induced Holliday junctions. *Cell Rep.*, **5**, 207–215.
9. Interthal,H. and Heyer,W.D. (2000) MUS81 encodes a novel helix-hairpin-helix protein involved in the response to UV- and methylation-induced DNA damage in Saccharomyces cerevisiae. *Mol. Gen. Genet.*, **263**, 812–827.
10. Ip,S.C., Rass,U., Blanco,M.G., Flynn,H.R., Skehel,J.M. and West,S.C. (2008) Identification of Holliday junction resolvases from humans and yeast. *Nature*, **456**, 357–361.
11. Kaliraman,V., Mullen,J.R., Fricke,W.M., Bastin-Shanower,S.A. and Brill,S.J. (2001) Functional overlap between Sgs1-Top3 and the Mms4-Mus81 endonuclease. *Genes Dev.*, **15**, 2730–2740.
12. Munoz,I.M., Hain,K., Declais,A.C., Gardiner,M., Toh,G.W., Sanchez-Pulido,L., Heuckmann,J.M., Toth,R., Macartney,T., Eppink,B. *et al.* (2009) Coordination of structure-specific nucleases by human SLX4/BTBD12 is required for DNA repair. *Mol. Cell*, **35**, 116–127.
13. Svendsen,J.M., Smogorzewska,A., Sowa,M.E., O′Connell,B.C., Gygi,S.P., Elledge,S.J. and Harper,J.W. (2009) Mammalian BTBD12/SLX4 assembles a Holliday junction resolvase and is required for DNA repair. *Cell*, **138**, 63–77.
14. Wechsler,T., Newman,S. and West,S.C. (2011) Aberrant chromosome morphology in human cells defective for Holliday junction resolution. *Nature*, **471**, 642–646.
15. Wyatt,H.D.M., Sarbajna,S., Matos,J. and West,S.C. (2013) Coordinated actions of SLX1-SLX4 and MUS81-EME1 for Holliday junction resolution in human cells. *Mol. Cell*, **52**, 234–247.
16. Manhart,C.M., Ni,X., White,M.A., Ortega,J., Surtees,J.A. and Alani,E. (2017) The mismatch repair and meiotic recombination endonuclease Mlh1-Mlh3 is activated by polymer formation and can cleave DNA substrates in trans. *PLoS Biol.*, **15**, e2001164.
17. Ranjha,L., Anand,R. and Cejka,P. (2014) The *Saccharomyces cerevisiae* Mlh1-Mlh3 heterodimer is an endonuclease that preferentially binds to Holliday junctions. *J. Biol. Chem.*, **289**, 5674–5686.
18. Rogacheva,M.V., Manhart,C.M., Chen,C., Guarne,A., Surtees,J. and Alani,E. (2014) Mlh1-Mlh3, a meiotic crossover and DNA mismatch repair factor, is a Msh2-Msh3-stimulated endonuclease. *J. Biol. Chem.*, **289**, 5664–5673.
19. Zakharyevich,K., Tang,S.M., Ma,Y.M. and Hunter,N. (2012) Delineation of joint molecule resolution pathways in meiosis identifies a crossover-specific resolvase. *Cell*, **149**, 334–347.
20. Kulkarni,D.S., Owens,S.N., Honda,M., Ito,M., Yang,Y., Corrigan,M.W., Chen,L., Quan,A.L. and Hunter,N. (2020) PCNA activates the MutLγ endonuclease to promote meiotic crossing over. *Nature*, **586**, 623–627.
21. Cannavo,E., Sanchez,A., Anand,R., Ranjha,L., Hugener,J., Adam,C., Acharya,A., Weyland,N., Aran-Guiu,X., Charbonnier,J.-B. *et al.* (2020) Regulation of the MLH1–MLH3 endonuclease in meiosis. *Nature*, **586**, 618–622.
22. Bennett,R.J. and West,S.C. (1996) Resolution of Holliday junctions in genetic recombination: RuvC protein nicks DNA at the point of strand exchange. *Proc. Natl. Acad. Sci. U.S.A.*, **93**, 12217–12222.
23. Bennett,R.J., Dunderdale,H.J. and West,S.C. (1993) Resolution of Holliday junctions by RuvC resolvase: Cleavage specificity and DNA distortion. *Cell*, **74**, 1021–1031.
24. Connolly,B., Parsons,C.A., Benson,F.E., Dunderdale,H.J., Sharples,G.J., Lloyd,R.G. and West,S.C. (1991) Resolution of Holliday junctions in vitro requires the Escherichia coli ruvC gene product. *Proc. Natl Acad. Sci. U.S.A.*, **88**, 6063–6067.
25. Górecka,K.M., Komorowska,W. and Nowotny,M. (2013) Crystal structure of RuvC resolvase in complex with Holliday junction substrate. *Nucleic Acids Res.*, **41**, 9945–9955.
26. Iwasaki,H., Takahagi,M., Shiba,T., Nakata,A. and Shinagawa,H. (1991) Escherichia coli RuvC protein is an endonuclease that resolves the Holliday structure. *EMBO J.*, **10**, 4381–4389.
27. Shah,R., Cosstick,R. and West,S.C. (1997) The RuvC dimer resolves Holliday junctions by a dual incision mechanism that involves base-specific contacts. *EMBO J.*, **16**, 1464–1472.
28. Mizuuchi,K., Kemper,B., Hays,J. and Weisberg,R.A. (1982) T4 endonuclease VII cleaves Holliday structures. *Cell*, **29**, 357–365.
29. Lilley,D.M.J. and Kemper,B. (1984) Cruciform-resolvase interactions in supercoiled DNA. *Cell*, **36**, 413–422.
30. Giraud-Panis,M.J.E. and Lilley,D.M.J. (1997) Near simultaneous DNA cleavage by the subunits of the junction-resolving enzyme T4 endonuclease VII. *EMBO J.*, **16**, 2528–2534.
31. Birkenbihl,R.P. and Kemper,B. (2002) High affinity of endonuclease VII for the Holliday structure containing one nick ensures productive resolution. *J. Mol. Biol.*, **321**, 21–28.
32. de Massy,B., Weisberg,R.A. and Studier,F.W. (1987) Gene 3 endonuclease of bacteriophage T7 resolves conformationally branched structures in double-stranded DNA. *J. Mol. Biol.*, **193**, 359–376.
33. Duckett,D.R., Murchie,A.I.H., Diekmann,S., Von Kitzing,E., Kemper,B. and Lilley,D.M.J. (1988) The structure of the Holliday junction and its resolution. *Cell*, **55**, 79–89.
34. Hadden,J.M., Declais,A.C., Carr,S.B., Lilley,D.M.J. and Phillips,S.E.V. (2007) The structural basis of Holliday junction resolution by T7 endonuclease. *Nature*, **449**, 621–624.
35. Kleff,S. and Kemper,B. (1988) Initiation of heteroduplex loop repair by T4-encoded endonuclease VII in vitro. *EMBO J.*, **7**, 1527–1535.
36. White,M.F. and Lilley,D.M.J. (1996) The structure-selectivity and sequence-preference of the junction-resolving enzyme Cce1 of Saccharomyces cerevisiae. *J. Mol. Biol.*, **257**, 330–341.
37. White,M.F. and Lilley,D.M.J. (1997) Characterization of a Holliday junction-resolving enzyme from Schizosaccharomyces pombe. *Mol. Cell. Biol.*, **17**, 6465–6471.
38. Whitby,M.C. and Dixon,J. (1997) A new Holliday junction resolving enzyme from *Schizosaccharomyces pombe* that is homologous to Cce1 from *Saccharomyces cerevisiae*. *J. Mol. Biol.*, **272**, 509–522.
39. Oram,M., Keeley,A. and Tsaneva,I. (1998) Holliday junction resolvase in Schizosaccharomyces pombe has identical endonuclease activity to the Cce1 homolog Ydc2. *Nucleic Acids Res.*, **26**, 594–601.
40. Chan,Y.W. and West,S. (2015) GEN1 promotes Holliday junction resolution by a coordinated nick and counter-nick mechanism. *Nucleic Acids Res.*, **43**, 10882–10892.
41. Fogg,J.M. and Lilley,D.M.J. (2000) Ensuring productive resolution by the junction-resolving enzyme RuvC: large enhancement of the second-strand cleavage rate. *Biochemistry*, **39**, 16125–16134.

Downloaded from https://academic.oup.com/nar/article/50/1/259/6470689 by Irene Ruiz user on 01 July 2022

42. Fogg,J.M., Schofield,M.J., Declais,A.C. and Lilley,D.M.J. (2000) Yeast resolving enzyme CCE1 makes sequential cleavages in DNA junctions within the lifetime of the complex. *Biochemistry*, **39**, 4082–4089.
43. Wyatt,H.D.M. and West,S.C. (2014) Holliday Junction Resolvases. *Cold Spring Harb. Perspect. Biol.*, **6**, a023192.
44. Furukawa,F., Kimura,M., ishibashi,T., Mori,Y., Hashimoto,J. and Sakaguchi,K. (2003) OsSEND-1: a new RAD2 nuclease family member in higher plants. *Plant Mol. Biol.*, **51**, 59–70.
45. Ishikawa,G., Kanai,Y., Takata,K., Takeuchi,R., Shimanouchi,K., Ruike,T., Furukawa,T., Kimura,S. and Sakaguchi,K. (2004) DmGEN, a novel RAD2 family endo-exonuclease from Drosophila melanogaster. *Nucleic Acids Res.*, **32**, 6251–6259.
46. Moritoh,S., Miki,D., Akiyama,M., Kawahara,M., Izawa,T., maki,H. and Shimamoto,K. (2005) RNAi-mediated silencing of OsGEN-L (OsGEN-like), a new member of the Rad2/XPG nuclease family, causes male sterility by defect of microspore development in rice. *Plant Cell Physiol.*, **46**, 699–715.
47. Bauknecht,M. and Kobbe,D. (2014) AtGEN1 and AtSEND1, two paralogs in Arabidopsis, possess holliday junction resolvase activity. *Plant Physiol.*, **166**, 202–216.
48. Freeman,A.D.J., Liu,Y., Déclais,A.-C., Gartner,A. and Lilley,D.M.J. (2014) GEN1 from a *Thermophilic fungus* is functionally closely similar to non-eukaryotic junction-resolving enzymes. *J. Mol. Biol.*, **426**, 3946–3959.
49. Bailly,A.P., Freeman,A., Hall,J., Declais,A.C., Alpi,A., Lilley,D.M.J., Ahmed,S. and Gartner,A. (2010) The *Caenorhabditis elegans* homolog of Gen1/Yen1 resolvases links DNA damage signaling to DNA double-strand break repair. *PLos Genet.*, **6**, e1001025.
50. Lee,S.-H., Princz,L.N., Klügel,M.F., Habermann,B., Pfander,B. and Biertümpfel,C. (2015) Human Holliday junction resolvase GEN1 uses a chromodomain for efficient DNA recognition and cleavage. *eLife*, **4**, e12256.
51. Lieber,M.R. (1997) The Fen-1 family of structure-specific nucleases in eukaryotic DNA replication, recombination and repair. *Bioessays*, **19**, 233–240.
52. Liu,Y., Freeman,A.D.J., Déclais,A.-C., Wilson,T.J., Gartner,A. and Lilley,D.M.J. (2015) Crystal structure of a eukaryotic GEN1 resolving enzyme bound to DNA. *Cell Rep.*, **13**, 2565–2575.
53. Bellendir,S.P., Rognstad,D.J., Morris,L.P., Zapotoczny,G., Walton,W.G., Redinbo,M.R., Ramsden,D.A., Sekelsky,J. and Erie,D.A. (2017) Substrate preference of Gen endonucleases highlights the importance of branched structures as DNA damage repair intermediates. *Nucleic Acids Res.*, **45**, 5333–5348.
54. Chan,Y.W. and West,S.C. (2014) Spatial control of the GEN1 Holliday junction resolvase ensures genome stability. *Nat. Commun.*, **5**, 4844.
55. Kanai,Y., Ishikawa,G., Takeuchi,R., Ruike,T., Nakamura,R., Ihara,A., Ohashi,T., Takata,K., Kimura,S. and Sakaguchi,K. (2007) DmGEN shows a flap endonuclease activity, cleaving the blocked-flap structure and model replication fork. *FEBS J.*, **274**, 3914–3927.
56. Rass,U., Compton,S.A., Matos,J., Singleton,M.R., Ip,S.C., Blanco,M.G., Griffith,J.D. and West,S.C. (2010) Mechanism of Holliday junction resolution by the human GEN1 protein. *Genes Dev.*, **24**, 1559–1569.
57. Shah Punatar,R., Martin,M.J., Wyatt,H.D.M., Chan,Y.W. and West,S.C. (2017) Resolution of single and double Holliday junction recombination intermediates by GEN1. *Proc. Natl. Acad. Sci. U.S.A.*, **114**, 443–450.
58. Yang,Y., Ishino,S., Yamagami,T., Kumamaru,T., Satoh,H. and Ishino,Y. (2012) The OsGEN-L protein from *Oryza sativa* possesses Holliday junction resolvase activity as well as 5′-flap endonuclease activity. *J. Biochem.*, **151**, 317–327.
59. Agmon,N., Yovel,M., Harari,Y., Liefshitz,B. and Kupiec,M. (2011) The role of Holliday junction resolvases in the repair of spontaneous and induced DNA damage. *Nucleic Acids Res.*, **39**, 7009–7019.
60. Blanco,M.G., Matos,J., Rass,U., Ip,S.C. and West,S.C. (2010) Functional overlap between the structure-specific nucleases Yen1 and Mus81-Mms4 for DNA-damage repair in S. cerevisiae. *DNA Repair Amst*, **9**, 394–402.
61. Ho,C.K., Mazón,G., Lam,A.F. and Symington,L.S. (2010) Mus81 and Yen1 promote reciprocal exchange during mitotic recombination to maintain genome integrity in budding yeast. *Mol. Cell*, **40**, 988–1000.
62. Johnson,R.E., Kovvali,G.K., Prakash,L. and Prakash,S. (1998) Role of yeast Rth1 nuclease and its homologs in mutation avoidance, DNA repair, and DNA replication. *Curr. Genet.*, **34**, 21–29.
63. Tay,Y.D. and Wu,L. (2010) Overlapping roles for Yen1 and Mus81 in cellular Holliday junction processing. *J. Biol. Chem.*, **285**, 11427–11432.
64. García-Luis,J. and Machín,F. (2014) Mus81-Mms4 and Yen1 resolve a novel anaphase bridge formed by noncanonical Holliday junctions. *Nat. Commun.*, **5**, 5652.
65. Matos,J., Blanco,M.G., Maslen,S., Skehel,J.M. and West,S.C. (2011) Regulatory control of the resolution of DNA recombination intermediates during meiosis and mitosis. *Cell*, **147**, 158–172.
66. de Muyt,A., Jessop,L., Kolar,E., Sourirajan,A., Chen,J., Dayani,Y. and Lichten,M. (2012) BLM helicase ortholog Sgs1 is a central regulator of meiotic recombination intermediate metabolism. *Mol. Cell*, **46**, 43–53.
67. Falquet,B., Ölmezer,G., Enkner,F., Klein,D., Challa,K., Appanah,R., Gasser,S.M. and Rass,U. (2020) Disease-associated DNA2 nuclease–helicase protects cells from lethal chromosome under-replication. *Nucleic Acids Res.*, **48**, 7265–7278.
68. Ölmezer,G., Levikova,M., Klein,D., Falquet,B., Fontana,G.A., Cejka,P. and Rass,U. (2016) Replication intermediates that escape Dna2 activity are processed by Holliday junction resolvase Yen1. *Nat. Commun.*, **7**, 13157.
69. Blanco,M.G., Matos,J. and West,S.C. (2014) Dual control of Yen1 nuclease activity and cellular localization by Cdk and Cdc14 prevents genome instability. *Mol. Cell*, **54**, 94–106.
70. Eissler,C.L., Mazón,G., Powers,B.L., Savinov,S.N., Symington,L.S. and Hall,M.C. (2014) The Cdk/Cdc14 module controls activation of the Yen1 Holliday junction resolvase to promote genome stability. *Mol. Cell*, **54**, 80–93.
71. Kosugi,S., Hasebe,M., Tomita,M. and Yanagawa,H. (2009) Systematic identification of cell cycle-dependent yeast nucleocytoplasmic shuttling proteins by prediction of composite motifs. *Proc. Natl. Acad. Sci. U.S.A.*, **106**, 10171–10176.
72. Talhaoui,I., Bernal,M., Mullen,J.R., Dorison,H., Palancade,B., Brill,S.J. and Mazón,G. (2018) Slx5-Slx8 ubiquitin ligase targets active pools of the Yen1 nuclease to limit crossover formation. *Nat. Commun.*, **9**, 5016.
73. Alonso-Ramos,P., Álvarez-Melo,D., Strouhalova,K., Pascual-Silva,C., Garside,G.B., Arter,M., Bermejo,T., Grigaitis,R., Wettstein,R., Fernández-Díaz,M. *et al.* (2021) The Cdc14 Phosphatase Controls Resolution of Recombination Intermediates and Crossover Formation during Meiosis. *Int. J. Mol. Sci.* **22**, 9811.
74. Arter,M., Hurtado-Nieves,V., Oke,A., Zhuge,T., Wettstein,R., Fung,J.C., Blanco,M.G. and Matos,J. (2018) Regulated crossing-over requires inactivation of Yen1/GEN1 resolvase during meiotic prophase I. *Dev. Cell*, **45**, 785–800.
75. Bittmann,J., Grigaitis,R., Galanti,L., Amarell,S., Wilfling,F., Matos,J. and Pfander,B. (2020) An advanced cell cycle tag toolbox reveals principles underlying temporal control of structure-selective nucleases. *eLife*, **9**, e52459.
76. Elango,R., Sheng,Z., Jackson,J., DeCata,J., Ibrahim,Y., Pham,N.T., Liang,D.H., Sakofsky,C.J., Vindigni,A., Lobachev,K.S. *et al.* (2017) Break-induced replication promotes formation of lethal joint molecules dissolved by Srs2. *Nat. Commun.*, **8**, 1790.
77. Grigaitis,R., Ranjha,L., Wild,P., Kasaciunaite,K., Ceppi,I., Kissling,V., Henggeler,A., Susperregui,A., Peter,M., Seidel,R. *et al.* (2020) Phosphorylation of the RecQ helicase Sgs1/BLM controls its DNA unwinding activity during meiosis and mitosis. *Dev. Cell*, **53**, 706–723.
78. Matos,J., Blanco,M.G. and West,S.C. (2013) Cell-cycle kinases coordinate the resolution of recombination intermediates with chromosome segregation. *Cell Rep.*, **4**, 76–86.
79. Michel,A.H., Hatakeyama,R., Kimmig,P., Arter,M., Peter,M., Matos,J., De Virgilio,C. and Kornmann,B. (2017) Functional mapping of yeast genomes by saturated transposition. *eLife*, **6**, e23570.
80. Wild,P., Susperregui,A., Piazza,I., Dörig,C., Oke,A., Arter,M., Yamaguchi,M., Hilditch,A.T., Vuina,K., Chan,K.C. *et al.* (2019) Network rewiring of homologous recombination enzymes during mitotic proliferation and meiosis. *Mol. Cell*, **75**, 859–874.

Downloaded from https://academic.oup.com/nar/article/50/1/259/6470689 by Irene Ruiz user on 01 July 2022

81. Mumberg,D., Muller,R. and Funk,M. (1995) Yeast vectors for the controlled expression of heterologous proteins in different genetic backgrounds. *Gene*, **156**, 119–122.
82. Carreira,R., Aguado,F.J., Lama-Diaz,T. and Blanco,M.G. (2021) Holliday junction resolution. *Methods Mol. Biol.*, **2153**, 169–185.
83. The UniProt Consortium (2021) UniProt: the universal protein knowledgebase in 2021. *Nucleic Acids Res.*, **49**, D480–D489.
84. Sievers,F., Wilm,A., Dineen,D., Gibson,T.J., Karplus,K., Li,W., Lopez,R., McWilliam,H., Remmert,M., Söding,J. *et al.* (2011) Fast, scalable generation of high-quality protein multiple sequence alignments using clustal omega. *Mol. Syst. Biol.*, **7**, 539.
85. Jumper,J., Evans,R., Pritzel,A., Green,T., Figurnov,M., Ronneberger,O., Tunyasuvunakool,K., Bates,R., Žídek,A., Potapenko,A. *et al.* (2021) Highly accurate protein structure prediction with AlphaFold. *Nature*, **596**, 583–589.
86. Osman,F., Dixon,J., Doe,C.L. and Whitby,M.C. (2003) Generating crossovers by resolution of nicked Holliday junctions: a role of Mus81-Eme1 in meiosis. *Mol. Cell*, **12**, 761–774.
87. Schwartz,E.K. and Heyer,W.D. (2011) Processing of joint molecule intermediates by structure-selective endonucleases during homologous recombination in eukaryotes. *Chromosoma*, **120**, 109–127.
88. Marsolier-Kergoat,M.-C., Khan,M.M., Schott,J., Zhu,X. and Llorente,B. (2018) Mechanistic view and genetic control of DNA recombination during meiosis. *Mol. Cell*, **70**, 9–20.
89. Machín,F. (2020) Implications of metastable nicks and nicked Holliday junctions in processing joint molecules in mitosis and meiosis. *Genes*, **11**, 1498.
90. Osman,F., Gaskell,L. and Whitby,M.C. (2009) Efficient second strand cleavage during Holliday junction resolution by RuvC requires both increased junction flexibility and an exposed 5′-phosphate. *PLoS One*, **4**, e5347.
91. West,S.C. (1997) Processing of recombination intermediates by the RuvABC proteins. *Annu. Rev. Genet.*, **31**, 213–244.
92. Lilley,D.M.J. (2000) Structures of helical junctions in nucleic acids. *Quat. Rev. Biophys.*, **33**, 109–159.
93. Bennett,R.J. and West,S.C. (1995) RuvC protein resolves Holliday junctions via cleavage of the continuous (non-crossover) strands. *Proc. Natl Acad. Sci. U.S.A.*, **92**, 5635–5639.
94. Bennett,R.J. and West,S.C. (1995) Structural analysis of the RuvC-Holliday junction complex reveals an unfolded junction. *J. Mol. Biol.*, **252**, 213–226.
95. Komori,K., Sakae,S., Shinagawa,H., Morikawa,K. and Ishino,Y. (1999) A Holliday junction resolvase from Pyrococcus furiosus: Functional similarity to Escherichia coli RuvC provides evidence for conserved mechanism of homologous recombination in Bacteria, Eukarya, and Archaea. *Proc. Natl Acad. Sci. U.S.A.*, **96**, 8873–8878.
96. Komori,K., Sakae,S., Fujikane,R., Morikawa,K., Shinagawa,H. and Ishino,Y. (2000) Biochemical characterization of the Hjc Holliday junction resolvase of *Pyrococcus furiosus*. *Nucleic Acids Res.*, **28**, 4544–4551.
97. Mueller,J.E., Kemper,B., Cunningham,R.P., Kallenbach,N.R. and Seeman,N.C. (1988) T4 endonuclease VII cleaves the crossover strands of Holliday junction analogs. *Proc. Natl. Acad. Sci. U.S.A.*, **85**, 9441–9445.
98. Lilley,D.M.J. (2017) Holliday junction-resolving enzymes—structures and mechanisms. *FEBS Lett.*, **591**, 1073–1082.
99. Gough,G.W. and Lilley,D.M.J. (1985) DNA bending induced by cruciform formation. *Nature*, **313**, 154–156.
100. Liu,Y., Freeman,A.D., Déclais,A.-C. and Lilley,D.M.J. (2018) A monovalent ion in the DNA binding interface of the eukaryotic junction-resolving enzyme GEN1. *Nucleic Acids Res.*, **46**, 11089–11098.
101. Lanz,M.C., Yugandhar,K., Gupta,S., Sanford,E.J., Faça,V.M., Vega,S., Joiner,A., Fromme,J.C., Yu,H. and Smolka,M.B. (2021) In-depth and 3-dimensional exploration of the budding yeast phosphoproteome. *EMBO reports*, **22**, e51121.
102. Sobhy,M.A., Bralić,A., Raducanu,V.-S., Takahashi,M., Tehseen,M., Rashid,F., Zaher,M.S. and Hamdan,S.M. (2019) Resolution of the Holliday junction recombination intermediate by human GEN1 at the single-molecule level. *Nucleic Acids Res.*, **47**, 1935–1949.
103. Bauer,S.L., Chen,J. and Åström,S.U. (2019) Helicase/SUMO-targeted ubiquitin ligase Uls1 interacts with the Holliday junction resolvase Yen1. *PLoS One*, **14**, e0214102.
104. Lorenz,A., West,S.C. and Whitby,M.C. (2010) The human Holliday junction resolvase GEN1 rescues the meiotic phenotype of a Schizosaccharomyces pombe mus81 mutant. *Nucleic Acids Res.*, **38**, 1866–1873.
105. Harrington,J.J. and Lieber,M.R. (1994) The characterization of a mammalian DNA structure specific endonuclease. *EMBO J.*, **13**, 1235–1246.
106. Murante,R.S., Huang,L., Turchi,J.J. and Bambara,R.A. (1994) The calf 5′- to 3′-exonuclease is also an endonuclease with both activities dependent on primers annealed upstream of the point of cleavage. *J. Biol. Chem.*, **269**, 1191–1196.
107. Lee,B.I. and Wilson,D.M. (1999) The RAD2 domain of human exonuclease 1 exhibits 5′ to 3′ exonuclease and flap structure-specific endonuclease activities. *J. Biol. Chem.*, **274**, 37763–37769.
108. Neelsen,K.J. and Lopes,M. (2015) Replication fork reversal in eukaryotes: from dead end to dynamic response. *Nat. Rev. Mol. Cell Biol.*, **16**, 207–220.

Downloaded from https://academic.oup.com/nar/article/50/1/259/6470689 by Irene Ruiz user on 01 July 2022